EUROPEAN ORGANIZATION FOR NUCLEAR RESEARCH (CERN)

CERN-EP-2021-272
2022/02/15

CMS-HIG-21-013

First evidence for off-shell production of the Higgs boson and measurement of its width

The CMS Collaboration*

Abstract

The first evidence for off-shell Higgs boson production is reported in the final state with two Z bosons decaying into either four charged leptons (muons or electrons), or two charged leptons and two neutrinos, and a measurement of the Higgs boson width is performed. Results are based on data from the CMS experiment at the LHC at a center-of-mass energy of 13 TeV, corresponding to an integrated luminosity of up to 140 fb^{-1}. The total rate of off-shell Higgs boson production beyond the Z boson pair production threshold, relative to its standard model expectation, is constrained to the interval [0.0061, 2.0] at 95% confidence level. The scenario with no off-shell production is excluded at 99.97% confidence level (3.6 standard deviations). The width of the Higgs boson is extracted as $\Gamma_{\mathrm{H}} = 3.2^{+2.4}_{-1.7}\,\text{MeV}$, in agreement with the standard model expectation of 4.1 MeV. The data are also used to set new constraints on anomalous Higgs boson couplings to W and Z boson pairs.

Submitted to Nature Physics

*See Appendix A for the list of collaboration members

The standard model (SM) of particle physics provides an elegant explanation for the masses and interactions of fundamental particles. These are fermions, which are the building blocks of ordinary matter, and gauge bosons, which are the carriers of the fundamental electroweak (EW) and strong forces. In addition, the SM postulates the existence of a quantum field responsible for the generation of the masses of fundamental particles through a phenomenon known as the Brout–Englert–Higgs mechanism. This field, known as the *Higgs field* [1–3], interacts with other SM particles, thereby giving them mass, as well as with itself. The carrier of this field is a massive, scalar (spin-0) particle known as the Higgs (H) boson. Nearly half a century after its postulation, it was finally observed in 2012 with a mass m_{H} of around 125 GeV by the ATLAS and CMS Collaborations [4–6] at the CERN Large Hadron Collider (LHC). Given the unique role the H boson plays in the SM, detailed studies of its properties are a major goal of particle physics.

Apart from mass, another important property of a particle is its lifetime τ. Only a few fundamental particles are stable; others—including the H boson—exist only for a fleeting moment of time before disintegrating into other lighter species. As one of the foundational bases of quantum mechanics, the Heisenberg uncertainty principle [7] provides a direct connection between the lifetime of a particle and the uncertainty in its mass, a property known as the particle's width, Γ. Any unstable particle (often referred to as a *resonance*) has a finite lifetime, with shorter τ corresponding to broader Γ. The two quantities are related through the reduced Planck constant, $\hbar$, as $\Gamma = \hbar/\tau$. Even with perfect experimental resolution, the observed mass of such an unstable particle will not be constant across a series of measurements (e.g., of the invariant mass of its decay products). The possible mass values are distributed according to a characteristic relativistic Breit–Wigner distribution [8], which describes the shape of many resonant phenomena, with a nominal mass value corresponding to the maximum of the Breit–Wigner, and with the width parameter Γ. Particles are understood to be *on the mass shell* (on-shell) if their mass is close to the nominal mass value, and *off-shell* if their mass takes a value arbitrarily far away from the nominal mass. By the aforementioned property of the Breit–Wigner line shape, particles are generally more likely to be produced on-shell than off-shell when energy and momentum conservation allow it.

For relatively broad resonances, the width can be experimentally obtained by directly measuring the Breit–Wigner line shape, e.g., as was done in the case of the Z boson, measured to have a mass of $m_{\mathrm{Z}} = 91.2\,\mathrm{GeV}$ and a width of $\Gamma_{\mathrm{Z}} = 2.5\,\mathrm{GeV}$ at the CERN Large Electron Positron collider [9]. The H boson is heavier than the Z boson, and it is expected to live three orders of magnitude longer. Its theoretically predicted width for $m_{\mathrm{H}} \approx 125\,\mathrm{GeV}$ is $\Gamma_{\mathrm{H}} = 4.1\,\mathrm{MeV}$ [10], and any deviation from the SM prediction may indicate the existence of new physics. Nevertheless, the width is too small to be measured directly from the line shape because of the limited mass resolution of order 1 GeV achievable with the present LHC detectors. Another direct way of measuring the H boson width would be to measure its lifetime by means of its decay length and use the relationship $\Gamma_{\mathrm{H}} = \hbar/\tau_{\mathrm{H}}$, but its lifetime is still too short ($\tau_{\mathrm{H}} = 1.6 \times 10^{-22}\,\mathrm{s}$) to be detectable directly. The present experimental limit on this quantity is $\tau_{\mathrm{H}} < 1.9 \times 10^{-13}\,\mathrm{s}$ at 95% confidence level (CL) [11], which is nine orders of magnitude above the SM lifetime.

The value of Γ_{H} can nevertheless be extracted with much better precision through a combined measurement of on-shell and off-shell H boson production. In the decay of an H boson with $m_{\mathrm{H}} \approx 125\,\mathrm{GeV}$ to a pair of massive gauge bosons V (V = W or Z, with a nominal mass of around 80.4 or 91.2 GeV, respectively), the relationship $m_{\mathrm{V}} < m_{\mathrm{H}} < 2m_{\mathrm{V}}$ is satisfied. When the H boson is produced on-shell ($m_{\mathrm{VV}} \sim m_{\mathrm{H}}$), one of the V bosons must be off-shell in order to simultaneously satisfy four-momentum conservation and this mass relation. Once the H boson is produced off-shell with a large enough invariant mass $m_{\mathrm{VV}} > 2m_{\mathrm{V}}$ (off-shell H boson production region), the V bosons themselves are produced on-shell. Since the Breit–Wigner mass distribution of either the H or V boson maximizes at their respective nominal masses, the rate of off-shell H boson production above the V boson pair production threshold is enhanced with respect to what one would expect from the Breit–Wigner line shape of the H boson alone. It is expected that 10% of all proton-proton (pp) collision events with pp $\rightarrow$ H $\rightarrow$ VV in the SM [12] result in two on-shell V bosons. This enhancement is large enough to allow for a statistically significant measurement of off-shell H boson production.

The measurement of the higher part of the VV invariant mass spectrum can then be used to establish off-shell H boson production, and the ratio of off-shell to on-shell production rates allows for a measurement of Γ_{H} [13, 14]. For the rest of the discussion in this article, we concentrate on ZZ final states, i.e., H $\rightarrow$ ZZ. The CMS and ATLAS Collaborations have previously used this method to set upper limits on Γ_{H}, as low as 9.2 MeV at 95% CL [15, 16].

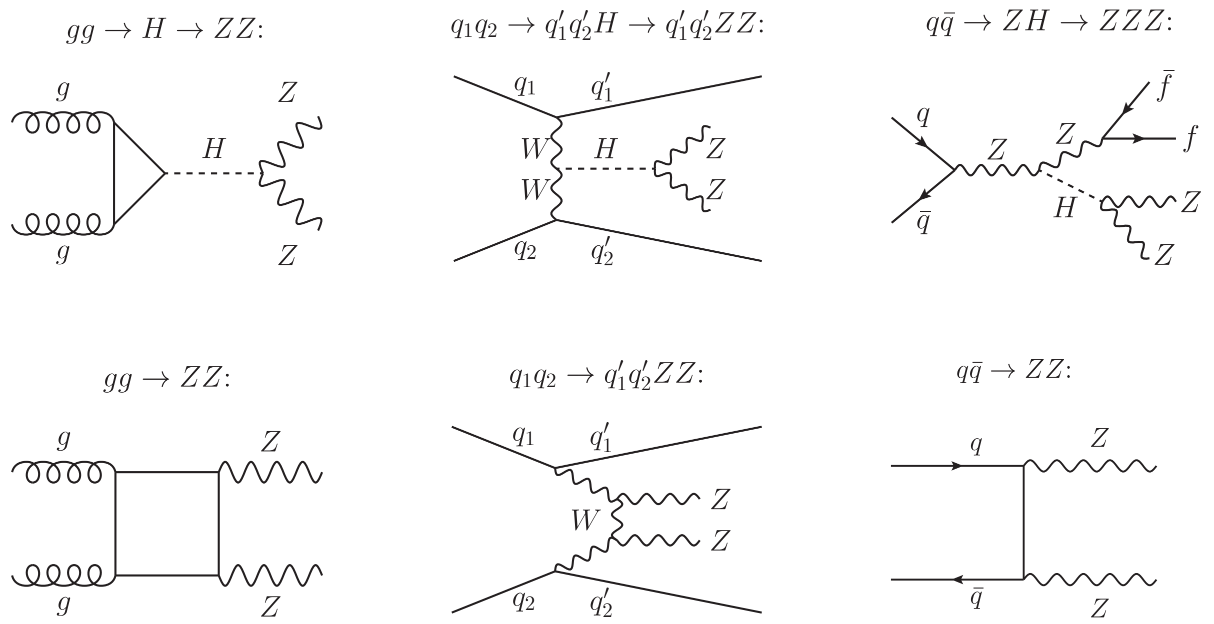

Figure 1: Tree-level Feynman diagrams for some of the most important contributions to ZZ production. Diagrams can be distinguished as those involving the H boson (top), and those that give rise to continuum ZZ production (bottom).

It is important to distinguish between two types of H boson production modes: the gluon fusion gg $\rightarrow$ H $\rightarrow$ ZZ process, where the H boson is produced via its couplings to fermions, and the EW processes, which involve HVV couplings. The top row of Fig. 1 shows the most dominant contributions for the gg (top left) process, and the EW processes of vector boson fusion (VBF, top center) and VH (top right). A more complete set of lowest order Feynman diagrams for the EW process are shown in Supplementary Figs. S1 and S2. Because different H boson couplings are involved in the gg and EW processes, we extract two signal strength parameters $\mu_{\mathrm{F}}^{\text{off-shell}}$ for the gg mode and $\mu_{\mathrm{V}}^{\text{off-shell}}$ for the EW modes, where the signal strengths are defined as the ratios of the measured cross sections to those predicted in the SM. We also consider an overall signal strength parameter $\mu^{\text{off-shell}}$ with different assumptions on the ratio $R_{\mathrm{V,F}}^{\text{off-shell}} = \mu_{\mathrm{V}}^{\text{off-shell}} / \mu_{\mathrm{F}}^{\text{off-shell}}$.

A major challenge arises from the fact that there are other sources of ZZ pairs in the SM (continuum ZZ production), see for example the bottom row of Fig. 1. These continuum contributions, particularly those from q$\bar{\mathrm{q}}$ $\rightarrow$ ZZ, are typically much larger than the contribution from off-shell H $\rightarrow$ ZZ. In addition, some of the amplitudes from continuum ZZ processes interfere destructively with the H boson amplitudes [12, 17–21] because they share the same initial and final states. For example, the amplitudes in the first and second columns of Fig. 1 interfere with each other, but the amplitude on the bottom right panel does not interfere with any of the others. These interference effects need to be included to keep the computed pp $\rightarrow$ ZZ cross section finite in the SM [17–20]. Figure 2 displays the interplay between the H boson production modes and the interfering continuum amplitudes, illustrating the growing importance of their destructive interference as m_{ZZ} grows in the two final states included in the analysis, ZZ $\rightarrow 2\ell 2\nu$ and ZZ $\rightarrow 4\ell$.

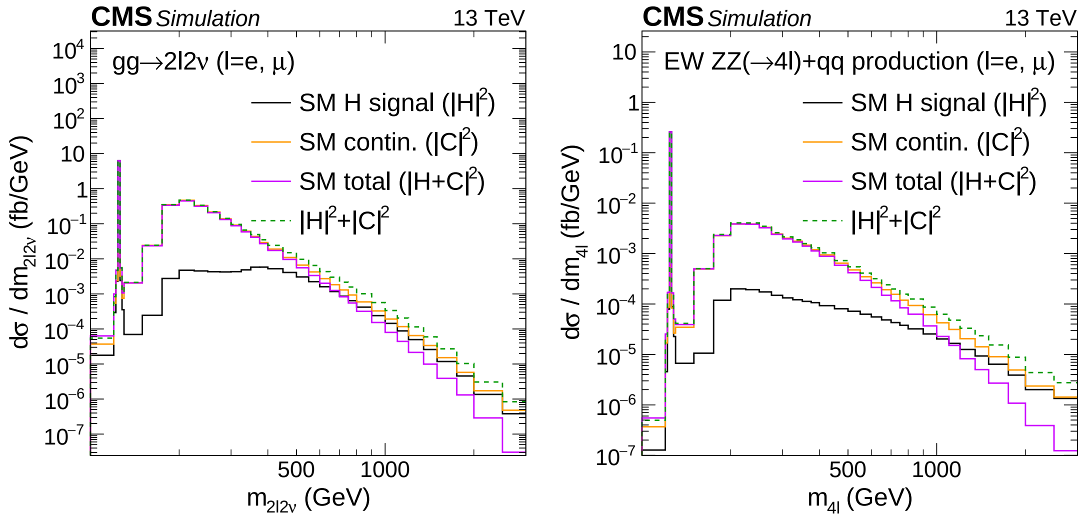

Figure 2: Standard model calculations of the $m_{2\ell 2\nu}$ (left) and $m_{4\ell}$ (right) distributions for the gg $\rightarrow 2\ell 2\nu$ and EW ZZ$(\rightarrow 4\ell) +$ qq processes. These processes involve H boson and interfering continuum contributions, shown in black and gold, respectively. The dashed green curve represents their direct sum without the interference, and the solid magenta curve represents the sum with interference included. Note that the interference is destructive, and its importance grows as the mass increases. Calculations for the gg $\rightarrow 4\ell$ and EW ZZ$(\rightarrow 2\ell 2\nu) +$ qq processes exhibit similar qualitative properties.

In this article, we study off-shell H boson decays to ZZ $\rightarrow 2\ell 2\nu$, and on-shell as well as off-shell H boson decays to ZZ $\rightarrow 4\ell$ ($\ell = \mu$ or e), using a sample of pp collisions at 13 TeV collected by the CMS experiment at the LHC. The selection and analysis of the off-shell ZZ $\rightarrow 2\ell 2\nu$ data sample is described in detail in this article, and it is based on data collected between 2016 and 2018, corresponding to an integrated luminosity of 138 fb^{-1}. For the ZZ $\rightarrow 4\ell$ mode, the analysis starts from previously published CMS off-shell (2016 and 2017 data sets, 78 fb^{-1} [16]) and on-shell (2015 [16, 22] and 2016–2018 [23] data sets, 2.3 fb^{-1} and 138 fb^{-1}, respectively) results.

Information on the off-shell signal strengths, Γ_H, and constraints on possible beyond-the-SM (BSM) anomalous couplings are extracted from combined fits over several kinematic distributions of the selected $2\ell 2\nu$ and 4ℓ events. While off-shell events are the ones solely used to establish the presence of off-shell H boson production, the measurement of Γ_H relies on the combination of on-shell and off-shell data.

Because of the presence of neutrinos, the H boson mass cannot be precisely reconstructed in the H $\rightarrow 2\ell 2\nu$ final state. Thus, on-shell information can only be extracted from the 4ℓ mode. This combination of 4ℓ and $2\ell 2\nu$ data enables the measurement of Γ_H with a precision of $\sim$50%.

The measurement improves the upper limit on τ_{H} by eight orders of magnitude compared to the direct constraint from Ref. [11]. The inclusion of the $2\ell 2\nu$ data also allows the lower limits on $\mu_{\mathrm{V}}^{\text{off-shell}}$ to reach within $\sim$65% of its best fit value, compared to the weaker constraints from 4ℓ data alone, which reach within $\sim$90% of the 4ℓ-only best fit value [16].

The m_{ZZ} line shape is sensitive to the potential presence of anomalous HVV couplings [10, 11, 16, 24–26]. Thus, BSM physics could affect the ratio of off-shell to on-shell H boson production rates, and therefore the measurement of Γ_{H}. We test the effect of these couplings on the Γ_{H} measurement and constrain the contribution from these couplings themselves. In parametrizing these anomalous HVV contributions, we adopt the formalism of Ref. [16], with real couplings a_2, a_3, and $1/\Lambda_1^2$ (denoted generically as a_i), where a_2 and a_3 are the coefficients of generic CP-conserving and CP-violating higher dimensional operators, respectively, while $1/\Lambda_1^2$ is the first-order term in the expansion of a SM-like tensor structure with a dipole form factor in the invariant masses of the two Z bosons. Finally, we note that throughout this work, we assume that the gluon fusion loop amplitudes do not receive new physics contributions beyond the SM prediction.

$2\ell 2\nu$ analysis considerations

The $2\ell 2\nu$ analysis is based on the reconstruction of $\mathrm{Z} \to \ell\ell$ decays in the presence of another Z boson decaying to neutrinos, which escape detection. The momentum of the undetected Z boson transverse with respect to the pp collision axis can be measured through an imbalance across all remaining particles, i.e., missing transverse momentum ($p_{\mathrm{T}}^{\text{miss}}$ or $\vec{p}_{\mathrm{T}}^{\text{miss}}$ in vector form). Thus, the analysis requires large $p_{\mathrm{T}}^{\text{miss}}$ as the signature of a $\mathrm{Z} \to \nu\nu$.

The event selection is sensitive to the tail of the instrumental $p_{\mathrm{T}}^{\text{miss}}$ resolution in $\mathrm{pp} \to \mathrm{Z}$+jets events (i.e., Drell–Yan, or DY in short), which constitutes an important reducible background. This contribution is estimated through a study of a data control region (CR) of γ+jets events in which $p_{\mathrm{T}}^{\text{miss}}$ is purely instrumental, just as it is in DY.

Processes such as $\mathrm{pp} \to \mathrm{t\bar{t}}$ and $\mathrm{pp} \to \mathrm{WW}$ result in dilepton final states of same ($\mathrm{e^+e^-}$ and $\mu^+\mu^-$) and opposite flavor ($\mathrm{e}^{\pm}\mu^{\mp}$ and $\mathrm{e}^{\mp}\mu^{\pm}$) with the same probability and the same kinematic properties. Thus, the background contribution to the $2\ell 2\nu$ signal, which includes two leptons of the same flavor, is estimated from an opposite-flavor $\mathrm{e}\mu$ CR.

The other backgrounds, which are $\mathrm{q\bar{q}} \to \mathrm{ZZ}$, $\mathrm{q\bar{q}'} \to \mathrm{WZ}$ with $\mathrm{W} \to \ell\nu$ when the lepton is undetected, and the small contribution from Z boson production in association with t quarks, are estimated from simulation. However, a third CR of trilepton events that consists mostly of $\mathrm{q\bar{q}'} \to \mathrm{WZ}$ events is included as part of the $2\ell 2\nu$ data set in order to constrain the $\mathrm{q\bar{q}'} \to \mathrm{WZ}$ background with one lost lepton and, most importantly, the very large $\mathrm{q\bar{q}} \to \mathrm{ZZ}$ background. The ability to constrain $\mathrm{q\bar{q}} \to \mathrm{ZZ}$ from $\mathrm{q\bar{q}'} \to \mathrm{WZ}$ is based on the similarity in the physics of these two processes.

Further details on event selection, kinematic observables, and the methods to estimate the different contributions for the aforementioned CRs are discussed in the Methods section.

$2\ell 2\nu$ kinematic observables

The analysis of off-shell H boson events is based on m_{ZZ}. This quantity can be computed from the fully reconstructed momenta in the 4ℓ final state as the invariant mass of the 4ℓ system, $m_{4\ell}$. However, because of the undetected neutrinos, we can only use the transverse mass $m_{\mathrm{T}}^{\mathrm{ZZ}}$, defined below, as a proxy for m_{ZZ} in the $2\ell 2\nu$ final state. First, we identify $\vec{p}_{\mathrm{T}}^{\text{miss}}$ as the transverse momentum vector of the Z boson decaying into neutrinos. Since there is no information on the longitudinal momenta of the neutrinos, m_T^{ZZ} is then computed as the invariant mass of the ZZ pair with all longitudinal momenta set to zero. This results in a variable with a distribution that peaks at m_{ZZ}, with a long tail towards lower values. The definition of m_T^{ZZ} is

$$\left(m_T^{ZZ}\right)^2 = \left[\sqrt{p_T^{\ell\ell 2} + m_{\ell\ell}{}^2} + \sqrt{p_T^{miss 2} + m_Z{}^2}\right]^2 - \left|\vec{p}_T^{\,\ell\ell} + \vec{p}_T^{\,miss}\right|^2,$$

where $\vec{p}_T^{\,\ell\ell}$ and $m_{\ell\ell}$ are the dilepton transverse momentum vector and invariant mass, respectively, and m_Z, the Z boson pole mass, is taken to be 91.2 GeV [27].

A second kinematic quantity to characterize $2\ell 2\nu$ events is p_T^{miss}, which provides good discrimination against the DY background. Finally, in events with at least two jets, we use matrix element (MELA [26]) kinematic discriminants that distinguish the VBF process from the gg process or SM backgrounds. These discriminants are the same $\mathcal{D}_{2jet}^{VBF}$-type kinematic discriminants used in Refs. [16, 23], and are based on the four-momenta of the H boson and the two jets leading in p_T. More details on these discriminants are provided in the Methods section.

Data interpretation

The results for the off-shell signal strength parameters $\mu_F^{off\text{-}shell}$, $\mu_V^{off\text{-}shell}$, and $\mu^{off\text{-}shell}$, and the H boson width Γ_H are extracted from binned extended maximum likelihood fits over several kinematic distributions following the parametrization in Ref. [16]. Over different data periods and event categories, a total of 117 multidimensional distributions are used in the fit: 42 for off-shell $2\ell 2\nu$ data, which includes 18 distributions from the trilepton WZ CR, and 18 and 57 for off-shell and on-shell 4ℓ data, respectively.

Depending on the number of jets (N_j), the $2\ell 2\nu$ data sample is binned in m_T^{ZZ} and p_T^{miss} ($N_j < 2$), or m_T^{ZZ}, p_T^{miss}, and the $\mathcal{D}_{2jet}^{VBF}$-type kinematic discriminants ($N_j \geq 2$). For the 4ℓ samples, the binning is in $m_{4\ell}$ and MELA discriminants, which are sensitive to differences between the H boson signal and continuum ZZ production, or the interfering amplitudes, or anomalous HVV couplings. These variables are listed in Table II of Ref. [16] for 4ℓ off-shell data, under 'Scheme 2' in Table IV of Ref. [23] for on-shell 2016-2018 data, and in Table 1 of Ref. [16] for on-shell 2015 data.

Theoretical uncertainties in the kinematic distributions include the simulation of extra jets, which are up to 20% depending on N_j, and the quantum chromodynamic (QCD) running scale and parton distribution function (PDF) uncertainties in the cross section calculation, which are up to 30% and 20%, respectively, depending on the process, and m_T^{ZZ} or $m_{4\ell}$. These are particularly important in the gg process that cannot be constrained by the trilepton WZ CR. Theory uncertainties also include those associated with the EW corrections to the $q\overline{q} \to$ ZZ and WZ processes, which reach 20% at masses around 1 TeV [28, 29].

Experimental uncertainties include uncertainties in the lepton reconstruction and trigger efficiency (typically 1% per lepton), the integrated luminosity (between 1.2% and 2.5%, depending on the data-taking period [30–32]), and the jet energy scale and resolution [33], which affect the counting of jets, as well as the reconstruction of the VBF discriminants.

Results

A representative distribution of m_T^{ZZ}, integrated over all N_j, is shown for $2\ell 2\nu$ events on the left panel of Fig. 3. Finer details in terms of N_j and the various contributions to the event sample are displayed in Supplementary Fig. S4. Also shown on the right panel of Fig. 3 is a representative distribution of $m_{4\ell}$ from the combined off-shell 4ℓ events.

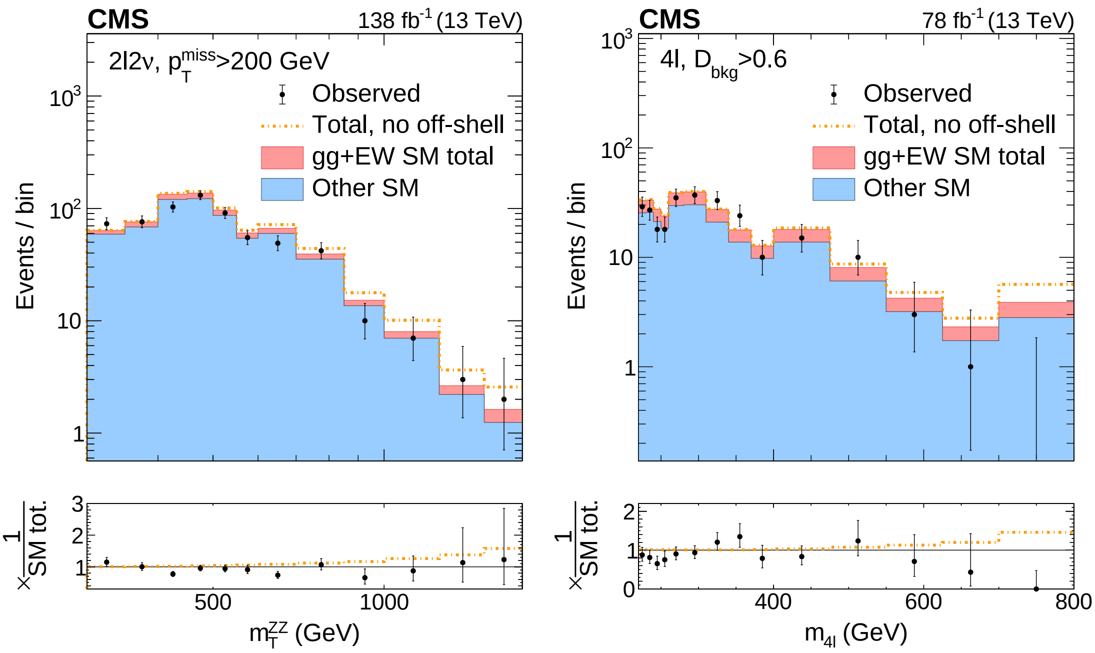

Figure 3: Distributions of m_T^{ZZ} in the $2\ell2\nu$ (left) and $m_{4\ell}$ in the 4ℓ (right) off-shell signal regions. The stacked histograms display the different predicted contributions after a fit to the data with SM couplings. The gold dot-dashed line shows the distribution after a fit to the no off-shell ($\Gamma_H = 0$ MeV) hypothesis. The black points show the observed data, which is consistent with the prediction with SM couplings within one standard deviation. The last bins contain the overflow. The requirements on p_T^{miss} in $2\ell2\nu$ events, and the $\mathcal{D}_{bkg}$-type kinematic discriminants (see Table II of Ref. [16]) in 4ℓ events are applied in order to enhance the H boson signal contribution. The values of integrated luminosity displayed correspond to those included in the off-shell analyses of each final state. The bottom pads show the ratio of the data or dashed histograms to the stacked histogram.

The constraints on $\mu_F^{\text{off-shell}}$, $\mu_V^{\text{off-shell}}$, $\mu^{\text{off-shell}}$, and Γ_H are summarized in Table 1. In summarizing the constraints, we show the "observed" results, i.e., those extracted from our data, as well as the "expected" ones, i.e., the results that we expect to obtain based on the SM and our initial prediction for event selection efficiencies, background expectations, and systematic uncertainties. Differences in the two set of results are found to be consistent with statistical fluctuations in the data.

The profile likelihood scans over the $\mu_F^{\text{off-shell}}$ and $\mu_V^{\text{off-shell}}$ plane are shown on the left panel of Fig. 4, and the profile likelihood scans over these parameters individually can be found in Supplementary Fig. S8. The scans over Γ_H are displayed in the right panel of Fig. 4. These scans always include information from the 4ℓ on-shell data, and the three cases displayed correspond to adding the 4ℓ off-shell data alone, adding the $2\ell2\nu$ off-shell data alone, or adding both.

The no off-shell scenario with $\mu^{\text{off-shell}} = 0$, or $\Gamma_H = 0$ MeV is excluded at 99.97% CL (3.6 standard deviations) in the full combination. Constraints on Γ_H are found to be stable within 1 MeV (0.1 MeV) for the upper (lower) limits when the presence of anomalous HVV couplings are tested. More results on anomalous H boson couplings to W and Z boson pairs can be found in the Methods section, and all results are tabulated in the HEPData record for this analysis [34].

Table 1: Summary of results on the off-shell signal strengths and Γ_H. The various fit conditions are indicated in the column labeled "Cond.": Results for $\mu^{\text{off-shell}}$ are with $R^{\text{off-shell}}_{V,F}$ either unconstrained (u) or $= 1$, and constraints on $\mu^{\text{off-shell}}_F$ and $\mu^{\text{off-shell}}_V$ are shown with the other signal strength unconstrained. Results for Γ_H (in units of MeV) are obtained with the on-shell signal strengths unconstrained, and the different conditions listed for this quantity reflect which off-shell final states are combined with on-shell 4ℓ data. The expected central values (not shown) are either unity or $\Gamma_H = 4.1\,\text{MeV}$.

Param.	Cond.	Observed 68% | 95% CL	Expected 68% | 95% CL
$\mu^{\text{off.}}_F$	$\mu^{\text{off.}}_V$ (u)	$0.62^{+0.68}_{-0.45}$ | $^{+1.38}_{-0.614}$	$^{+1.1}_{-0.99998}$ | < 3.0
$\mu^{\text{off.}}_V$	$\mu^{\text{off.}}_F$ (u)	$0.90^{+0.9}_{-0.59}$ | $^{+2.0}_{-0.849}$	$^{+2.0}_{-0.89}$ | < 4.5
$\mu^{\text{off.}}$	$R^{\text{off.}}_{V,F} = 1$	$0.74^{+0.56}_{-0.38}$ | $^{+1.06}_{-0.61}$	$^{+1.0}_{-0.84}$ | $^{+1.7}_{-0.9914}$
	$R^{\text{off.}}_{V,F}$ (u)	$0.62^{+0.68}_{-0.45}$ | $^{+1.38}_{-0.6139}$	$^{+1.1}_{-0.99996}$ | $^{+2.0}_{-0.99999}$
Γ_H	$2\ell2\nu + 4\ell$	$3.2^{+2.4}_{-1.7}$ | $^{+5.3}_{-2.7}$	$^{+4.0}_{-3.48}$ | $^{+7.2}_{-4.065}$
Γ_H	$2\ell2\nu$	$3.1^{+3.4}_{-2.1}$ | $^{+7.3}_{-2.91}$	$^{+5.1}_{-3.67}$ | $^{+9.1}_{-4.099}$
Γ_H	4ℓ	$3.8^{+3.8}_{-2.7}$ | $^{+8.0}_{-3.727}$	$^{+5.1}_{-4.047}$ | < 13.8

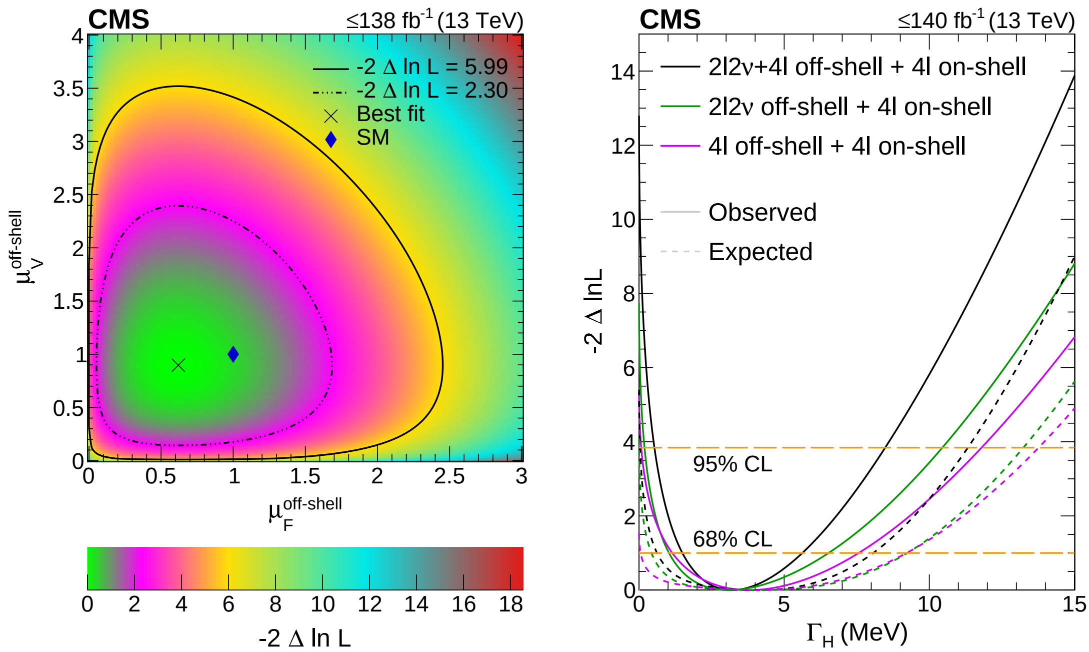

Figure 4: Left panel: Two-parameter likelihood scan of $\mu^{\text{off-shell}}_F$ and $\mu^{\text{off-shell}}_V$. The dot-dashed and dashed contours enclose the 68% ($-2\Delta\ln\mathcal{L} = 2.30$) and 95% ($-2\Delta\ln\mathcal{L} = 5.99$) CL regions. The cross marks the minimum, and the blue diamond marks the SM expectation. The integrated luminosity reaches only up to $138\,\text{fb}^{-1}$ as on-shell 4ℓ events are not included in performing this scan. Right panel: The observed (solid) and expected (dashed) one-parameter likelihood scans over Γ_H. Scans are shown for the combination of 4ℓ on-shell data with 4ℓ off-shell (magenta) or $2\ell2\nu$ off-shell data (green) alone, or with both data sets (black). The horizontal lines indicate the 68% ($-2\Delta\ln\mathcal{L} = 1.00$) and 95% ($-2\Delta\ln\mathcal{L} = 3.84$) CL regions. The integrated luminosity reaches up to $140\,\text{fb}^{-1}$ as on-shell 4ℓ events are included in performing these scans. The exclusion of the no off-shell hypothesis is consistent with 3.6 standard deviations on both panels.

Summary

To summarize, by analyzing ZZ events produced in proton-proton collisions at 13 TeV, we report the first evidence for off-shell H boson production, excluding the no off-shell scenario at 99.97% confidence level (3.6 standard deviations). We perform a measurement of its total width, $\Gamma_{\mathrm{H}} = 3.2^{+2.4}_{-1.7}$ MeV, reflecting a precision of $\sim$50%, and set limits on anomalous H boson couplings to W and Z boson pairs. The constraint on Γ_{H} at 95% confidence level corresponds to $7.7 \times 10^{-23} < \tau_{\mathrm{H}} < 1.3 \times 10^{-21}$ s in terms of the H boson lifetime, and improves the current upper limit from the direct lifetime measurement by eight orders of magnitude. These results are based on a new analysis of the $2\ell 2\nu$ final state, combined with previously published results for $\mathrm{ZZ} \to 4\ell$ using up to 140 fb^{-1} of proton-proton collisions collected with the CMS detector at the LHC between 2015 and 2018. Our measurements are consistent with the SM expectations.

References

[1] F. Englert and R. Brout, "Broken symmetry and the mass of gauge vector mesons", *Phys. Rev. Lett.* **13** (1964) 321, doi:10.1103/PhysRevLett.13.321.

[2] P. W. Higgs, "Broken symmetries and the masses of gauge bosons", *Phys. Rev. Lett.* **13** (1964) 508, doi:10.1103/PhysRevLett.13.508.

[3] G. S. Guralnik, C. R. Hagen, and T. W. B. Kibble, "Global conservation laws and massless particles", *Phys. Rev. Lett.* **13** (1964) 585, doi:10.1103/PhysRevLett.13.585.

[4] ATLAS Collaboration, "Observation of a new particle in the search for the Standard Model Higgs boson with the ATLAS detector at the LHC", *Phys. Lett. B* **716** (2012) 1, doi:10.1016/j.physletb.2012.08.020, arXiv:1207.7214.

[5] CMS Collaboration, "Observation of a new boson at a mass of 125 GeV with the CMS experiment at the LHC", *Phys. Lett. B* **716** (2012) 30, doi:10.1016/j.physletb.2012.08.021, arXiv:1207.7235.

[6] CMS Collaboration, "Observation of a new boson with mass near 125 GeV in pp collisions at $\sqrt{s} = 7$ and 8 TeV", *JHEP* **06** (2013) 081, doi:10.1007/JHEP06(2013)081, arXiv:1303.4571.

[7] W. Heisenberg, "Über den anschaulichen inhalt der quantentheoretischen kinematik und mechanik", *Z. Phys.* **43** (1927) 172, doi:10.1007/BF01397280.

[8] G. Breit and E. Wigner, "Capture of slow neutrons", *Phys. Rev.* **49** (1936) 519, doi:10.1103/PhysRev.49.519.

[9] ALEPH, DELPHI, L3, OPAL, SLD, LEP Electroweak Working Group, SLD Electroweak Group, SLD Heavy Flavour Group Collaboration, "Precision electroweak measurements on the Z resonance", *Phys. Rept.* **427** (2006) 257, doi:10.1016/j.physrep.2005.12.006, arXiv:hep-ex/0509008.

[10] LHC Higgs Cross Section Working Group, "Handbook of LHC Higgs cross sections: 4. Deciphering the nature of the Higgs sector", CERN Report CERN-2017-002-M, 2016. doi:10.23731/CYRM-2017-002, arXiv:1610.07922.

[11] CMS Collaboration, "Limits on the Higgs boson lifetime and width from its decay to four charged leptons", *Phys. Rev. D* **92** (2015) 072010, doi:10.1103/PhysRevD.92.072010, arXiv:1507.06656.

[12] N. Kauer and G. Passarino, "Inadequacy of zero-width approximation for a light Higgs boson signal", *JHEP* **08** (2012) 116, doi:10.1007/JHEP08(2012)116, arXiv:1206.4803.

[13] F. Caola and K. Melnikov, "Constraining the Higgs boson width with ZZ production at the LHC", *Phys. Rev. D* **88** (2013) 054024, doi:10.1103/PhysRevD.88.054024, arXiv:1307.4935.

[14] J. M. Campbell, R. K. Ellis, and C. Williams, "Bounding the Higgs width at the LHC using full analytic results for $gg \to e^-e^+\mu^-\mu^+$", *JHEP* **04** (2014) 060, doi:10.1007/JHEP04(2014)060, arXiv:1311.3589.

[15] ATLAS Collaboration, "Constraints on off-shell Higgs boson production and the Higgs boson total width in $ZZ \to 4\ell$ and $ZZ \to 2\ell 2\nu$ final states with the ATLAS detector", *Phys. Lett. B* **786** (2018) 223, doi:10.1016/j.physletb.2018.09.048, arXiv:1808.01191.

[16] CMS Collaboration, "Measurements of the Higgs boson width and anomalous HVV couplings from on-shell and off-shell production in the four-lepton final state", *Phys. Rev. D* **99** (2019) 112003, doi:10.1103/PhysRevD.99.112003, arXiv:1901.00174.

[17] C. H. Llewellyn Smith, "High-energy behavior and gauge symmetry", *Phys. Lett. B* **46** (1973) 233, doi:10.1016/0370-2693(73)90692-8.

[18] J. M. Cornwall, D. N. Levin, and G. Tiktopoulos, "Derivation of gauge invariance from high-energy unitarity bounds on the *S*-matrix", *Phys. Rev. D* **10** (1974) 1145, doi:10.1103/PhysRevD.10.1145. Erratum, doi:10.1103/PhysRevD.11.972.

[19] B. W. Lee, C. Quigg, and H. B. Thacker, "Weak interactions at very high-energies: the role of the Higgs boson mass", *Phys. Rev. D* **16** (1977) 1519, doi:10.1103/PhysRevD.16.1519.

[20] E. W. N. Glover and J. J. van der Bij, "Z boson pair production via gluon fusion", *Nucl. Phys. B* **321** (1989) 561, doi:10.1016/0550-3213(89)90262-9.

[21] F. Campanario, Q. Li, M. Rauch, and M. Spira, "ZZ+jet production via gluon fusion at the LHC", *JHEP* **06** (2013) 069, doi:10.1007/JHEP06(2013)069, arXiv:1211.5429.

[22] CMS Collaboration, "Constraints on anomalous Higgs boson couplings using production and decay information in the four-lepton final state", *Phys. Lett. B* **775** (2017) 1, doi:10.1016/j.physletb.2017.10.021, arXiv:1707.00541.

[23] CMS Collaboration, "Constraints on anomalous Higgs boson couplings to vector bosons and fermions in its production and decay using the four-lepton final state", *Phys. Rev. D* **104** (2021) 052004, doi:10.1103/PhysRevD.104.052004, arXiv:2104.12152.

[24] J. S. Gainer et al., "Beyond geolocating: Constraining higher dimensional operators in $H \to 4\ell$ with off-shell production and more", *Phys. Rev. D* **91** (2015) 035011, doi:10.1103/PhysRevD.91.035011, arXiv:1403.4951.

[25] C. Englert and M. Spannowsky, "Limitations and opportunities of off-shell coupling measurements", *Phys. Rev. D* **90** (2014) 053003, doi:10.1103/PhysRevD.90.053003, arXiv:1405.0285.

[26] A. V. Gritsan et al., "New features in the JHU generator framework: constraining Higgs boson properties from on-shell and off-shell production", *Phys. Rev. D* **102** (2020) 056022, doi:10.1103/PhysRevD.102.056022, arXiv:2002.09888.

[27] Particle Data Group, P. A. Zyla et al., "Review of Particle Physics", *PTEP* **2020** (2020) 083C01, doi:10.1093/ptep/ptaa104.

[28] A. Bierweiler, T. Kasprzik, and J. H. Kühn, "Vector-boson pair production at the LHC to $\mathcal{O}(\alpha^3)$ accuracy", *JHEP* **12** (2013) 071, doi:10.1007/JHEP12(2013)071, arXiv:1305.5402.

[29] A. Manohar, P. Nason, G. P. Salam, and G. Zanderighi, "How bright is the proton? A precise determination of the photon parton distribution function", *Phys. Rev. Lett.* **117** (2016) 242002, doi:10.1103/PhysRevLett.117.242002, arXiv:1607.04266.

[30] CMS Collaboration, "Precision luminosity measurement in proton-proton collisions at $\sqrt{s} = 13$ TeV in 2015 and 2016 at CMS", *Eur. Phys. J. C* **81** (2021) 800, doi:10.1140/epjc/s10052-021-09538-2, arXiv:2104.01927.

[31] CMS Collaboration, "CMS luminosity measurement for the 2017 data-taking period at $\sqrt{s} = 13$ TeV", CMS Physics Analysis Summary CMS-PAS-LUM-17-004, 2018.

[32] CMS Collaboration, "CMS luminosity measurement for the 2018 data-taking period at $\sqrt{s} = 13$ TeV", CMS Physics Analysis Summary CMS-PAS-LUM-18-002, 2019.

[33] CMS Collaboration, "Jet energy scale and resolution in the CMS experiment in pp collisions at 8 TeV", *JINST* **12** (2017) P02014, doi:10.1088/1748-0221/12/02/P02014, arXiv:1607.03663.

[34] CMS Collaboration. HEPData record for this analysis, 2022. doi:10.17182/hepdata.127288.

[35] CMS Collaboration, "The CMS experiment at the CERN LHC", *JINST* **3** (2008) S08004, doi:10.1088/1748-0221/3/08/S08004.

[36] CMS Collaboration, "The CMS trigger system", *JINST* **12** (2017) P01020, doi:10.1088/1748-0221/12/01/P01020, arXiv:1609.02366.

[37] CMS Collaboration, "Performance of the CMS muon detector and muon reconstruction with proton-proton collisions at $\sqrt{s} = 13$ TeV", *JINST* **13** (2018) P06015, doi:10.1088/1748-0221/13/06/P06015, arXiv:1804.04528.

[38] CMS Collaboration, "Electron and photon reconstruction and identification with the CMS experiment at the CERN LHC", *JINST* **16** (2021) P05014, doi:10.1088/1748-0221/16/05/P05014, arXiv:2012.06888.

[39] CMS Collaboration, "Description and performance of track and primary-vertex reconstruction with the CMS tracker", *JINST* **9** (2014) P10009, doi:10.1088/1748-0221/9/10/P10009, arXiv:1405.6569.

[40] CMS Collaboration, "Particle-flow reconstruction and global event description with the CMS detector", *JINST* **12** (2017) P10003, doi:10.1088/1748-0221/12/10/P10003, arXiv:1706.04965.

[41] CMS Collaboration, "Performance of missing transverse momentum reconstruction in proton-proton collisions at $\sqrt{s} = 13$ TeV using the CMS detector", *JINST* **14** (2019) P07004, doi:10.1088/1748-0221/14/07/P07004, arXiv:1903.06078.

[42] CMS Collaboration, "Performance of reconstruction and identification of τ leptons decaying to hadrons and ν_τ in pp collisions at $\sqrt{s} = 13$ TeV", *JINST* **13** (2018) P10005, doi:10.1088/1748-0221/13/10/P10005, arXiv:1809.02816.

[43] CMS Collaboration, "Measurements of inclusive W and Z cross sections in pp collisions at $\sqrt{s} = 7$ TeV", *JHEP* **01** (2011) 080, doi:10.1007/JHEP01(2011)080, arXiv:1012.2466.

[44] M. Cacciari, G. P. Salam, and G. Soyez, "FastJet user manual", *Eur. Phys. J. C* **72** (2012) 1896, doi:10.1140/epjc/s10052-012-1896-2, arXiv:1111.6097.

[45] CMS Collaboration, "Pileup mitigation at CMS in 13 TeV data", *JINST* **15** (2020) P09018, doi:10.1088/1748-0221/15/09/P09018, arXiv:2003.00503.

[46] E. Bols et al., "Jet flavour classification using DeepJet", *JINST* **15** (2020) 12012, doi:10.1088/1748-0221/15/12/P12012, arXiv:2008.10519.

[47] CMS Collaboration, "Missing transverse energy performance of the CMS detector", *JINST* **6** (2011) P09001, doi:10.1088/1748-0221/6/09/P09001, arXiv:1106.5048.

[48] S. Frixione, P. Nason, and C. Oleari, "Matching NLO QCD computations with parton shower simulations: the POWHEG method", *JHEP* **11** (2007) 070, doi:10.1088/1126-6708/2007/11/070, arXiv:0709.2092.

[49] P. Nason and C. Oleari, "NLO Higgs boson production via vector-boson fusion matched with shower in POWHEG", *JHEP* **02** (2010) 037, doi:10.1007/JHEP02(2010)037, arXiv:0911.5299.

[50] E. Bagnaschi, G. Degrassi, P. Slavich, and A. Vicini, "Higgs production via gluon fusion in the POWHEG approach in the SM and in the MSSM", *JHEP* **02** (2012) 088, doi:10.1007/JHEP02(2012)088, arXiv:1111.2854.

[51] G. Luisoni, P. Nason, C. Oleari, and F. Tramontano, "$HW^{\pm}/HZ$ + 0 and 1 jet at NLO with the POWHEG BOX interfaced to GoSam and their merging within MiNLO", *JHEP* **10** (2013) 083, doi:10.1007/JHEP10(2013)083, arXiv:1306.2542.

[52] M. Grazzini, S. Kallweit, and M. Wiesemann, "Fully differential NNLO computations with MATRIX", *Eur. Phys. J. C* **78** (2018) 537, doi:10.1140/epjc/s10052-018-5771-7, arXiv:1711.06631.

[53] R. Frederix and S. Frixione, "Merging meets matching in MC@NLO", *JHEP* **12** (2012) 061, doi:10.1007/JHEP12(2012)061, arXiv:1209.6215.

[54] J. Alwall et al., "Comparative study of various algorithms for the merging of parton showers and matrix elements in hadronic collisions", *Eur. Phys. J. C* **53** (2008) 473, doi:10.1140/epjc/s10052-007-0490-5, arXiv:0706.2569.

[55] T. Sjöstrand et al., "An introduction to PYTHIA 8.2", *Comput. Phys. Commun.* **191** (2015) 159, doi:10.1016/j.cpc.2015.01.024, arXiv:1410.3012.

[56] CMS Collaboration, "Event generator tunes obtained from underlying event and multiparton scattering measurements", *Eur. Phys. J. C* **76** (2016) 155, doi:10.1140/epjc/s10052-016-3988-x, arXiv:1512.00815.

[57] CMS Collaboration, "Extraction and validation of a new set of CMS PYTHIA8 tunes from underlying-event measurements", *Eur. Phys. J. C* **80** (2020) 4, doi:10.1140/epjc/s10052-019-7499-4, arXiv:1903.12179.

[58] NNPDF Collaboration, "Parton distributions for the LHC Run II", *JHEP* **04** (2015) 040, doi:10.1007/JHEP04(2015)040, arXiv:1410.8849.

[59] GEANT4 Collaboration, "GEANT4—a simulation toolkit", *Nucl. Instrum. Meth. A* **506** (2003) 250, doi:10.1016/S0168-9002(03)01368-8.

[60] CMS Collaboration, "Search for physics beyond the standard model in events with a Z boson, jets, and missing transverse energy in pp collisions at $\sqrt{s} = 7\,\text{TeV}$", *Phys. Lett. B* **716** (2012) 260, doi:10.1016/j.physletb.2012.08.026, arXiv:1204.3774.

Methods

Experimental setup

The CMS apparatus [35] is a multipurpose, nearly hermetic detector, designed to trigger on [36] and identify muons, electrons, photons, and charged or neutral hadrons [37–39]. A global reconstruction algorithm, particle-flow (PF) [40], combines the information provided by the all-silicon inner tracker and by the crystal electromagnetic and brass-scintillator hadron calorimeters (ECAL and HCAL, respectively), operating inside a 3.8 T superconducting solenoid, with data from gas-ionization muon detectors interleaved with the solenoid return yoke, to build jets, missing transverse momentum, tau leptons, and other physics objects [33, 41, 42]. In the following discussion up to likelihood scans, we will focus on the details of the $2\ell 2\nu$ analysis. Analysis details for the off-shell 4ℓ data can be found in Ref. [16], 2015 on-shell 4ℓ data in Refs. [16, 22], and 2016–2018 on-shell 4ℓ data in Ref. [23].

Physics objects

Events in the $2\ell 2\nu$ signal region, the $\mathrm{e}\mu$ CR, and the trilepton WZ CR are selected using single-lepton and dilepton triggers. The efficiencies of these selections are measured using orthogonal triggers, i.e., jet or $p_{\mathrm{T}}^{\mathrm{miss}}$ triggers, and events triggered on a third, isolated lepton, or a jet. They range between 78% and 100%, depending on the flavor of the leptons, p_{T}, and pseudorapidity (η) of the dilepton system, taking lower values at lower p_{T}. Photon triggers are used to collect events for the γ+jets CR. The photon trigger efficiency is measured using a tag-and-probe method [43] in $\mathrm{Z} \to \mathrm{ee}$ events, with one electron interpreted as a photon with tracks ignored, as well as through a study of $\ell\ell\gamma$ events. The efficiency is found to range from $\sim$55% at photon $p_{\mathrm{T}} = 55\,\mathrm{GeV}$ to $\sim$95% at photon $p_{\mathrm{T}} > 220\,\mathrm{GeV}$.

Jets are reconstructed using the anti-k_{T} algorithm [44] with a distance parameter of 0.4. Jet energies are corrected for instrumental effects, as well as for the contribution of particles originating from additional pp interactions (pileup). A multivariate technique is used to suppress jets from pileup interactions [45]. For the purpose of this analysis, we select jets of $p_{\mathrm{T}} > 30\,\mathrm{GeV}$ and $|\eta| < 4.7$, and they must be separated by $\Delta R = \sqrt{(\Delta\phi)^2 + (\Delta\eta)^2} > 0.4$, with ϕ being the azimuthal angle measured in radians, from a lepton or a photon of interest. Jets within $|\eta| < 2.5$ ($|\eta| < 2.4$ for 2016 data) can be identified as b jets using the DEEPJET algorithm [46] with a loose working point. The efficiency of this working point ranges between 75% and 95%, depending on p_{T}, η, and the data period.

The missing transverse momentum vector $\vec{p}_{\mathrm{T}}^{\mathrm{miss}}$ is estimated from the negative of the vector sum of the transverse momenta of all PF candidates. Dedicated algorithms [47] are used to eliminate events featuring cosmic ray contributions, beam-gas interactions, beam halo, or calorimetric noise.

The algorithms to reconstruct leptons are described in detail in Ref. [37] for muons and Ref. [38] for electrons. Muons are identified using a set of requirements on individual variables, while electrons are identified using a boosted decision tree algorithm. Leptons of interest in this analysis are expected to be isolated with respect to the activity in the rest of the event. A measure of isolation is computed from the flux of photons and hadrons reconstructed by the PF algorithm that are within a cone of $\Delta R < 0.3$ built around the lepton direction, including corrections from the contributions of pileup. We define loose and tight isolation requirements for muons (electrons) with $p_{\mathrm{T}} > 5\,\mathrm{GeV}$ and $|\eta| < 2.4$ ($|\eta| < 2.5$). The efficiency of loose selection for muons (electrons) ranges from $\sim$85% (65–75%, depending on η) at $p_{\mathrm{T}} = 5\,\mathrm{GeV}$ to $> 90\%$ ($> 85\%$) at $p_{\mathrm{T}} > 25\,\mathrm{GeV}$. The additional requirements for tight selections reduce efficiencies by

10–15%.

Photons are reconstructed from energy clusters in the ECAL not linked to charged tracks, with the exception of converted photons [38]. Their energies are corrected for shower containment in the ECAL crystals and energy loss due to conversions in the tracker with a multivariate regression. In this analysis, we consider photons with $p_{\mathrm{T}} > 20\,\mathrm{GeV}$ and $|\eta|$ up to 2.5, with requirements on shower shape and isolation used to identify isolated photons and separate them from hadronic jets. The selection requirements are tightened in the γ+jets CR, which leads to selection efficiencies in the range 50–75%, depending on p_{T} and η.

Event simulation

The signal Monte Carlo samples are generated for an undecayed H boson for gg, VBF, ZH, and WH productions using the POWHEG 2 [48–51] program at next-to-leading order (NLO) in QCD at various H boson pole masses, ranging from 125 GeV to 3 TeV. The generated H bosons are decayed to four-fermion final states through intermediate Z bosons using the JHUGEN [26] program, with versions between 6.9.8 and 7.4.0.

These samples are reweighted using MELA matrix elements following the prescription of Ref. [16] to obtain the final ZZ event sample, including the H boson contribution, the continuum, and their interference. The MELAANALYTICS package developed for Ref. [16] is used to automate matrix element computations and to account for the extra partons in the NLO simulation. The gg generation is rescaled with the next-to-NLO (NNLO) QCD K-factor, differential in m_{VV}, and an additional uniform K-factor of 1.10 for the next-to-NNLO cross section computed at $m_{\mathrm{H}} = 125\,\mathrm{GeV}$ [10].

The tree-level Feynman diagrams in Fig. 1 illustrate the complete set contributing to the gg $\to$ ZZ process on the leftmost top and bottom panels, and some of the diagrams contributing to the EW ZZ production associated with two fermions on the middle and top right panels. Supplementary Figs. S1 and S2 display the full set of diagrams for the EW process.

The $\mathrm{q\overline{q}} \to$ ZZ and WZ MC samples are also generated with POWHEG 2 applying EW NLO corrections for two on-shell Z and W bosons [28, 29], and NNLO QCD corrections as a function of m_{VV} [52]. The tree-level Feynman diagrams for these noninterfering continuum contributions are illustrated in Supplementary Fig. S3. Samples for the tZ+X processes, or other processes contributing to the CRs, are generated using MADGRAPH5_aMC@NLO at NLO or LO precision using the FxFx [53] or MLM [54] schemes, respectively, to match jets from matrix element calculations and parton shower.

The parton shower and hadronization are modeled with PYTHIA (8.205 or 8.230) [55], using tunes CUETP8M1 [56] for the 2015 and 2016 data sets, and CP5 [57] for the 2017 and 2018 periods. The PDFs are taken from NNPDF 3.0 [58] with QCD orders matching those of the cross section calculations. Finally, the detector response is simulated with the GEANT4 [59] package.

Signal region selection requirements

Events in the $2\ell 2\nu$ final state are required to have two opposite-sign, same-flavor leptons ($\mu^+\mu^-$ or $\mathrm{e^+e^-}$) satisfying tight isolation requirements with $p_{\mathrm{T}} > 25\,\mathrm{GeV}$, $m_{\ell\ell}$ within 15 GeV of m_{Z}, and $p_{\mathrm{T}}^{\ell\ell} > 55\,\mathrm{GeV}$. Additional requirements are imposed to reduce contributions from Z+jets and $\mathrm{t\overline{t}}$ processes as follows. Events with b-tagged jets, additional loosely isolated leptons of $p_{\mathrm{T}} > 5\,\mathrm{GeV}$, or additional loosely identified photons with $p_{\mathrm{T}} > 20\,\mathrm{GeV}$ are vetoed. To further improve the effectiveness of the lepton veto, events with isolated reconstructed tracks of $p_{\mathrm{T}} >$

10 GeV are removed. This requirement is also effective against one-prong τ decays.

The value of $p_{\mathrm{T}}^{\mathrm{miss}}$ is required to be > 125 GeV (> 140 GeV) for $N_{\mathrm{j}} < 2$ (≥ 2). Requirements are imposed on the unsigned azimuthal opening angles ($\Delta\phi$) between $\vec{p}_{\mathrm{T}}^{\mathrm{miss}}$ and other objects in the event in order to reduce contamination from $p_{\mathrm{T}}^{\mathrm{miss}}$ misreconstruction: $\Delta\phi_{\mathrm{miss}}^{\ell\ell} > 1.0$ between $\vec{p}_{\mathrm{T}}^{\mathrm{miss}}$ and $\vec{p}_{\mathrm{T}}^{\ell\ell}$, $\Delta\phi_{\mathrm{miss}}^{\ell\ell\text{+jets}} > 2.5$ between $\vec{p}_{\mathrm{T}}^{\mathrm{miss}}$ and $\vec{p}_{\mathrm{T}}^{\ell\ell} + \sum \vec{p}_{\mathrm{T}}^{\mathrm{j}}$, $\min \Delta\phi_{\mathrm{miss}}^{\mathrm{j}} > 0.25$ (0.50) between $\vec{p}_{\mathrm{T}}^{\mathrm{miss}}$ and $\vec{p}_{\mathrm{T}}^{\mathrm{j}}$ for $N_{\mathrm{j}} = 1$ ($N_{\mathrm{j}} \geq 2$), where $\vec{p}_{\mathrm{T}}^{\mathrm{j}}$ is the transverse momentum vector of a jet.

Finally, events are split into lepton flavor ($\mu\mu$ or ee) and jet multiplicity ($N_{\mathrm{j}} = 0, 1, \geq 2$) categories. The resulting event distributions are illustrated along the $m_{\mathrm{T}}^{\mathrm{ZZ}}$ observable in Supplementary Fig. S4.

Matrix element kinematic discriminants

In events with $N_{\mathrm{j}} \geq 2$, we use two MELA kinematic discriminants for the VBF process, $\mathcal{D}_{\mathrm{2jet}}^{\mathrm{VBF}}$ and $\mathcal{D}_{\mathrm{2jet}}^{\mathrm{VBF},a2}$ [16]. Each of these discriminants consists of a ratio of two matrix elements, or equivalently a ratio of event-by-event probability functions, expressed in terms of the four-momenta of the H boson and the two jets leading in p_{T}. The four-momentum of the H boson in the $2\ell 2\nu$ channel is approximated by taking the η of the $\mathrm{Z} \to 2\nu$ candidate, together with its sign, to be the same as that of the $\mathrm{Z} \to 2\ell$ candidate. This approximation is validated with Monte Carlo (MC) studies.

In both discriminants, one of matrix elements is always computed for the SM H boson production through gluon fusion. The remaining matrix element is computed for the SM VBF process in $\mathcal{D}_{\mathrm{2jet}}^{\mathrm{VBF}}$, so this discriminant improves the sensitivity to the EW H boson production. The $\mathcal{D}_{\mathrm{2jet}}^{\mathrm{VBF},a2}$ discriminant also computes the remaining matrix element for the VBF process, but under the a_2 HVV coupling hypothesis instead of the SM scenario. We find that this second discriminant brings additional sensitivity to SM backgrounds as well as being sensitive to the a_2 HVV coupling hypothesis by design. When anomalous HVV contributions are considered, the a_2 hypothesis used in the computation is replaced by the appropriate a_i hypothesis to optimize sensitivity for the coupling of interest.

Control regions

As already mentioned, Z+jets events can be a background to the $2\ell 2\nu$ signal selection. This can occur because of resolution effects in $p_{\mathrm{T}}^{\mathrm{miss}}$ and the large cross section for this process. Since γ+jets and Z+jets have similar properties, the Z+jets contributions at high $p_{\mathrm{T}}^{\mathrm{miss}}$ can be estimated from a γ+jets CR [60].

In this CR, all event selection requirements are the same as those on the signal region, except that the photon replaces the $\mathrm{Z} \to \ell\ell$ decay. The $m_{\mathrm{T}}^{\mathrm{ZZ}}$ kinematic variable is constructed using the photon p_{T} in place of $p_{\mathrm{T}}^{\ell\ell}$, and m_{Z} in place of $m_{\ell\ell}$. Only photons in the barrel region (i.e., $|\eta| < 1.44$) are considered for $N_{\mathrm{j}} < 2$ to eliminate beam halo events that can mimic the $\gamma + p_{\mathrm{T}}^{\mathrm{miss}}$ signature. Reweighting factors are extracted as a function of photon p_{T}, photon η (when $N_{\mathrm{j}} \geq 2$), and the number of observed pp collisions by matching the corresponding distributions in γ+jets sidebands at low $p_{\mathrm{T}}^{\mathrm{miss}}$ (< 125 GeV) to those of DY sidebands with the same requirement at each N_{j} category separately. These reweighting factors are then applied to the high-$p_{\mathrm{T}}^{\mathrm{miss}}$ γ+jets data sample.

Contributions to the γ+jets CR from events with genuine large $p_{\mathrm{T}}^{\mathrm{miss}}$ from the $\mathrm{Z}(\to \nu\nu)\gamma$, $\mathrm{W}(\to \ell\nu)\gamma$, and $\mathrm{W}(\to \ell\nu)$ + jets processes are subtracted in the final estimate of the instrumental

$p_{\mathrm{T}}^{\mathrm{miss}}$ background. The first two are estimated from simulation, where the Zγ contribution is corrected based on the observed rate of $\mathrm{Z}(\to \ell\ell) + \gamma$. The W + jets contribution is estimated from a single-electron sample selected with requirements similar to those in the γ+jets CR. Representative distributions for this estimate are shown in Supplementary Fig. S5.

Processes such as $\mathrm{pp} \to \mathrm{t\bar{t}}$ and $\mathrm{pp} \to \mathrm{WW}$, including nonresonant H boson contributions, can produce two leptons and large $p_{\mathrm{T}}^{\mathrm{miss}}$ without a resonant $\mathrm{Z} \to \ell\ell$ decay. The kinematic properties of the dilepton system in these processes is the same for any combination of lepton flavors e or μ. These nonresonant ee or $\mu\mu$ background processes are therefore estimated from an eμ CR. This CR is constructed applying the same requirements used in the signal selection except for the flavor of the leptons. Data events are reweighted to account for differences in trigger and reconstruction efficiencies between eμ, and ee or $\mu\mu$ final states. Representative distributions for this estimate are shown in Supplementary Fig. S6.

A third CR selects trilepton $\mathrm{q\bar{q}} \to \mathrm{WZ}$ events. These events are used to constrain the normalization and kinematic properties of the $\mathrm{q\bar{q}} \to \mathrm{ZZ}$ and WZ continuum contributions. The $\mathrm{Z} \to \ell\ell$ candidate is identified from the opposite-sign, same-flavor lepton pair with $m_{\ell\ell}$ closest to m_{Z}, and the value of $m_{\ell\ell}$ for this Z candidate is required to be within 15 GeV of m_{Z}. Trigger requirements are only placed on this Z candidate. The remaining lepton is identified as the lepton from the W decay (ℓ_{W}). The leading-p_{T} lepton from the Z decay is required to satisfy $p_{\mathrm{T}} > 30$ GeV, and the remaining leptons are required to satisfy $p_{\mathrm{T}} > 20$ GeV.

Similar to the signal region, requirements are imposed on the unsigned $\Delta\phi$ between $\vec{p}_{\mathrm{T}}^{\mathrm{miss}}$ and other objects in the event in order to reduce contamination from the DY and $\mathrm{q\bar{q}} \to \mathrm{Z}\gamma$ processes: $\Delta\phi_{\mathrm{miss}}^{\ell\ell} > 1.0$ between $\vec{p}_{\mathrm{T}}^{\mathrm{miss}}$ and $\vec{p}_{\mathrm{T}}^{\ell\ell}$ for the Z candidate, $\Delta\phi_{\mathrm{miss}}^{3\ell\text{+jets}} > 2.5$ between $\vec{p}_{\mathrm{T}}^{\mathrm{miss}}$ and $\vec{p}_{\mathrm{T}}^{3\ell} + \sum \vec{p}_{\mathrm{T}}^{\mathrm{j}}$, and $\min \Delta\phi_{\mathrm{miss}}^{\mathrm{j}} > 0.25$ between $\vec{p}_{\mathrm{T}}^{\mathrm{miss}}$ and $\vec{p}_{\mathrm{T}}^{\mathrm{j}}$.

The W boson transverse mass is defined through the vector transverse momentum of ℓ_{W}, $\vec{p}_{\mathrm{T}}^{\,\ell_{\mathrm{W}}}$, as $m_{\mathrm{T}}^{\ell_{\mathrm{W}}} = \sqrt{2(p_{\mathrm{T}}^{\ell_{\mathrm{W}}} p_{\mathrm{T}}^{\mathrm{miss}} - \vec{p}_{\mathrm{T}}^{\,\ell_{\mathrm{W}}} \cdot \vec{p}_{\mathrm{T}}^{\mathrm{miss}})}$, and additional requirements are imposed on $p_{\mathrm{T}}^{\mathrm{miss}}$ and $m_{\mathrm{T}}^{\ell_{\mathrm{W}}}$ in order to reduce contamination from the DY and $\mathrm{q\bar{q}} \to \mathrm{Z}\gamma$ processes further: $p_{\mathrm{T}}^{\mathrm{miss}} > 20$ GeV, $m_{\mathrm{T}}^{\ell_{\mathrm{W}}} > 20$ GeV (10 GeV) for $\ell_{\mathrm{W}} = \mu$ (e), and $\mathrm{A} \times m_{\mathrm{T}}^{\ell_{\mathrm{W}}} + p_{\mathrm{T}}^{\mathrm{miss}} > 120$ GeV, with A = 1.6 (4/3) for $\ell_{\mathrm{W}} = \mu$ (e). All other requirements on b-tagged jets, and additional leptons or photons are the same as those for the signal region.

The events are finally split into categories of the flavor of ℓ_{W} (μ or e) and jet multiplicity ($N_{\mathrm{j}} = 0, 1, \geq 2$), and binned in $m_{\mathrm{T}}^{\mathrm{WZ}}$, defined using the W boson mass $m_{\mathrm{W}} = 80.4$ GeV [27] as

$$\left(m_{\mathrm{T}}^{\mathrm{WZ}}\right)^2 = \left[\sqrt{p_{\mathrm{T}}^{\ell\ell\,2} + m_{\ell\ell}^{\,2}} + \sqrt{\left|\vec{p}_{\mathrm{T}}^{\mathrm{miss}} + \vec{p}_{\mathrm{T}}^{\,\ell_{\mathrm{W}}}\right|^2 + m_{\mathrm{W}}^{\,2}}\right]^2 - \left|\vec{p}_{\mathrm{T}}^{\,\ell\ell} + \vec{p}_{\mathrm{T}}^{\mathrm{miss}} + \vec{p}_{\mathrm{T}}^{\,\ell_{\mathrm{W}}}\right|^2.$$

Event distributions along $m_{\mathrm{T}}^{\mathrm{WZ}}$ from this CR are shown in Supplementary Fig. S7.

Likelihood scans

As mentioned in the discussion of data interpretation, the likelihood is constructed from several multidimensional distributions binned over the different event categories. Profile likelihood scans over $\mu_{\mathrm{F}}^{\text{off-shell}}$, $\mu_{\mathrm{V}}^{\text{off-shell}}$, $\mu^{\text{off-shell}}$, and Γ_{H} are shown in Supplementary Fig. S8. When testing the effects of anomalous HVV couplings, we perform fits to the data with all BSM couplings set to zero, except the one being tested, in the model to be fit. Because the only remaining degree of freedom is the ratio of these BSM couplings to the SM-like coupling, a_1, the probability densities are parametrized in terms of the effective, signed on-shell cross section fraction f_{ai} for each of the a_i coupling, where the sign of the phase of a_i relative to a_1 is absorbed into the definition of f_{ai} [23]. The constraints on Γ_H are found to be stable within 1 MeV (0.1 MeV) for the upper (lower) limits under the different anomalous HVV coupling conditions, and they are summarized in Table S1.

In addition, we provide a simplified illustration for the exclusion of the no off-shell hypothesis in Fig. S9. In this figure, the total number of events in each bin of the likelihood are compared from the $2\ell2\nu$ and 4ℓ off-shell regions for the fit of the data to the no off-shell ($N_{\text{no off-shell}}$) scenario, and the best fit ($N_{\text{best fit}}$). Events can then be rebinned over the ratio $N_{\text{no off-shell}}/(N_{\text{no off-shell}} + N_{\text{best fit}})$ extracted from each bin, and these rebinned distributions can then be compared at different Γ_H values. In particular, we compare the observed and expected event distributions over this ratio under the best fit scenario, and the scenario with no off-shell H boson production ($\Gamma_H = 0$ MeV), in order to illustrate which bins bring most sensitivity to the exclusion of the no off-shell scenario. The exclusion is noted to be most apparent from the last two bins displayed in this figure. We note, however, that the full power of the analysis ultimately comes from the different bins over the multidimensional likelihood, and that this figure only serves to condense the information for illustration.

When we perform separate likelihood scans over the three f_{ai} fractions, only the corresponding BSM parameter is allowed to be nonzero in the fit. Profile likelihood scans for f_{a2}, f_{a3} and $f_{\Lambda1}$ under different fit conditions are shown in Supplementary Fig. S10, and the summary of the allowed intervals at 68% and 95% CL is presented in Supplementary Table S2.

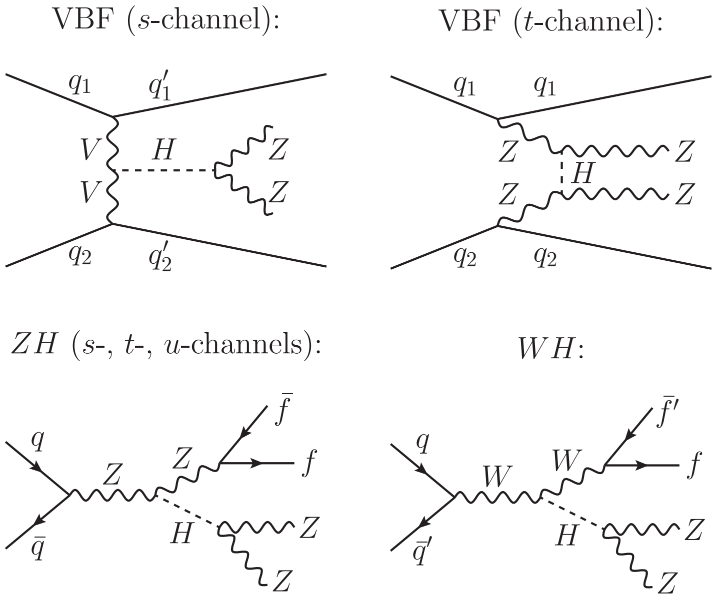

Figure S1: The tree-level Feynman diagrams contributing to the EW $ZZ + f\bar{f}$ production, where f refers to any ℓ, ν, or q, are shown for the H boson-mediated contributions. Diagrams featuring VBF production are grouped together in the upper row, and those featuring VH production are grouped in the lower row.

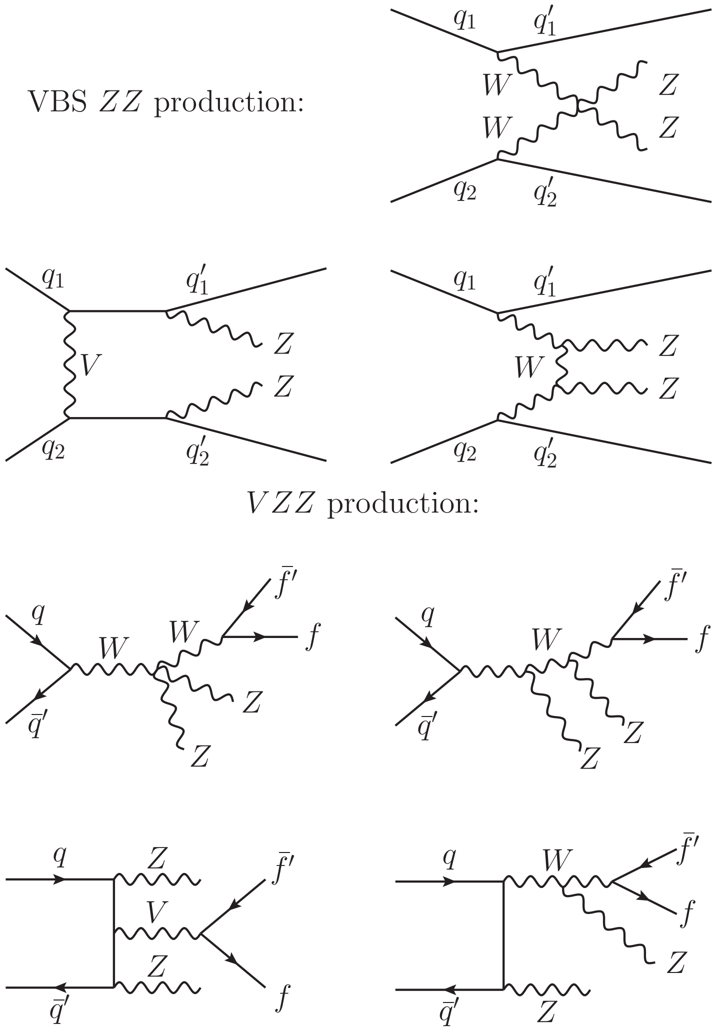

Figure S2: The tree-level Feynman diagrams contributing to the EW ZZ + ff production, where f refers to any ℓ, ν, or q, are shown for the continuum ZZ production contributions. Diagrams featuring vector boson scattering (VBS) production are grouped together in the upper half, and those featuring VZZ production are grouped in the lower half.

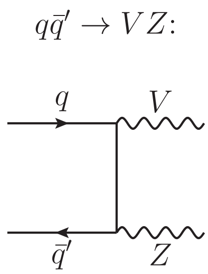

Figure S3: The Feynman diagrams contributing to the $q\overline{q} \to ZZ$ and $q\overline{q}' \to WZ$ processes at tree level are represented with a single diagram. These two processes constitute the major irreducible, noninterfering background contributions in the off-shell region.

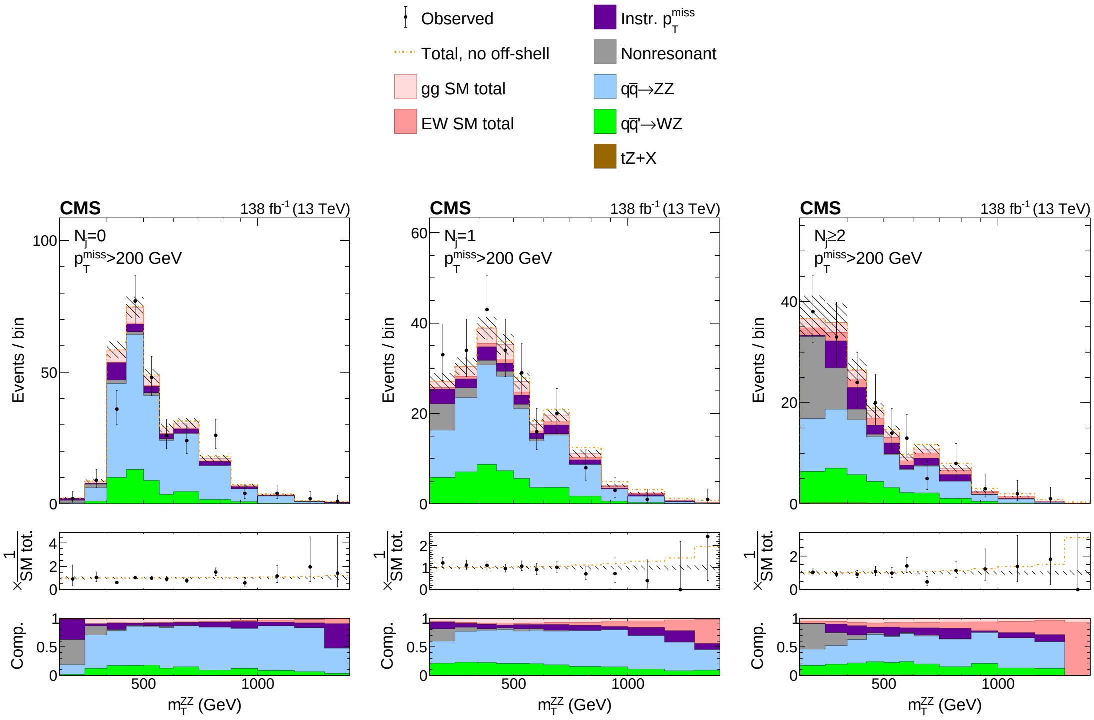

Figure S4: Postfit distributions of $m_{\mathrm{T}}^{\mathrm{ZZ}}$ in the $N_{\mathrm{j}} = 0$ (left), $= 1$ (middle), and ≥ 2 (right) categories of the $2\ell 2\nu$ signal region with a $p_{\mathrm{T}}^{\mathrm{miss}} > 200\,\mathrm{GeV}$ requirement to enrich H boson contributions. The color legend for the stacked or dot-dashed histograms is given above the plots. Postfit refers to individual fits of the data to the combined $2\ell 2\nu + 4\ell$ sample, assuming SM H boson parameters (stacked histogram) or no off-shell H boson production (dot-dashed gold line, equivalent to setting $\Gamma_{\mathrm{H}} = 0\,\mathrm{MeV}$). The middle pads show the ratio of the data or dashed histograms to the stacked histogram, and the lower pads show the relative contributions of each process in the stacked histogram. The rightmost bins contain the overflow.

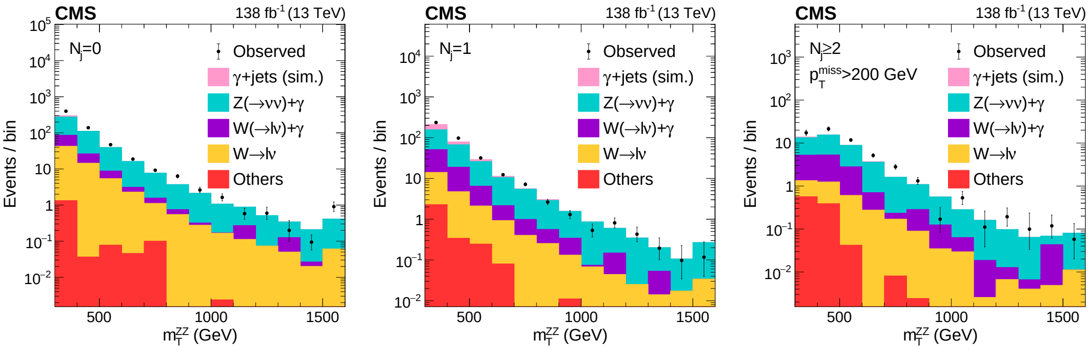

Figure S5: The distributions of $m_{\mathrm{T}}^{\mathrm{ZZ}}$ are shown from the γ+jets CR for the $N_{\mathrm{j}} = 0$, $N_{\mathrm{j}} = 1$, and $N_{\mathrm{j}} \geq 2$ categories from left to right. The requirement $p_{\mathrm{T}}^{\mathrm{miss}} > 200\,\mathrm{GeV}$ is applied in the $N_{\mathrm{j}} \geq 2$ category to focus on the region more sensitive to off-shell H boson production. The stacked histograms show the predictions for contributions with genuine, large $p_{\mathrm{T}}^{\mathrm{miss}}$, or the instrumental $p_{\mathrm{T}}^{\mathrm{miss}}$ background from the γ+jets simulation. The black points show the observed CR data. The distributions are reweighted with the $\gamma \to \ell\ell$ transfer factors extracted from the $p_{\mathrm{T}}^{\mathrm{miss}} < 125\,\mathrm{GeV}$ sidebands. The rightmost bins include the overflow. In these distributions, we find a discrepancy between the observed data and the predicted distributions because the reweighted γ+jets samples have inaccurate $p_{\mathrm{T}}^{\mathrm{miss}}$ response and the simulation is at LO in QCD. Therefore, we use the difference between the observed data and the genuine-$p_{\mathrm{T}}^{\mathrm{miss}}$ contributions to model the instrumental $p_{\mathrm{T}}^{\mathrm{miss}}$ background instead of using simulation for this estimate.

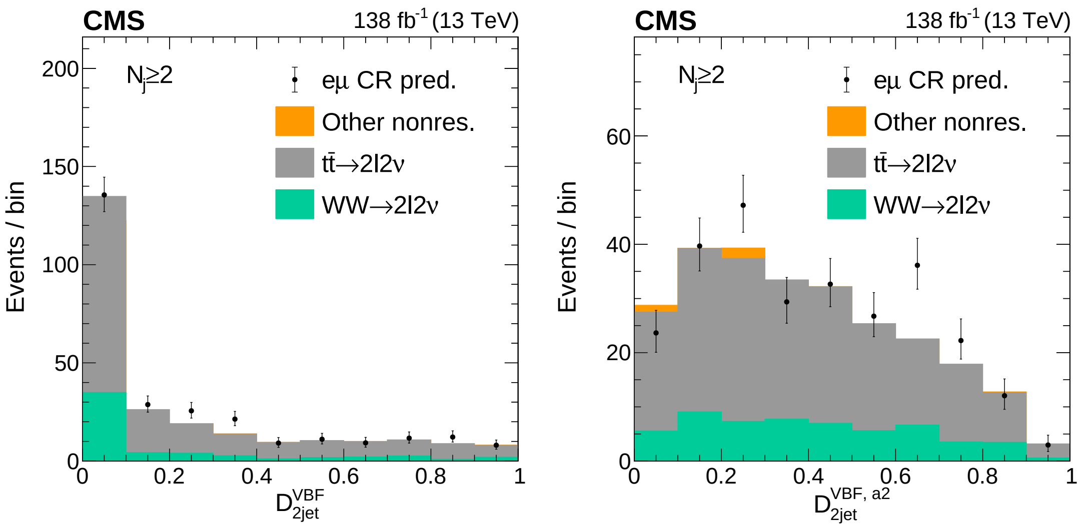

Figure S6: The distributions of the SM $\mathcal{D}_{\mathrm{2jet}}^{\mathrm{VBF}}$ (left) and $\mathcal{D}_{\mathrm{2jet}}^{\mathrm{VBF},a2}$ kinematic discriminants are shown in the $2\ell 2\nu$ signal region, $N_{\mathrm{j}} \geq 2$ category. The stacked histograms show the predictions from simulation, and the black points show the prediction from the eμ CR data. While only the data is used in the final estimate of the nonresonant background, we note that predictions from simulation already agree well with the data estimate.

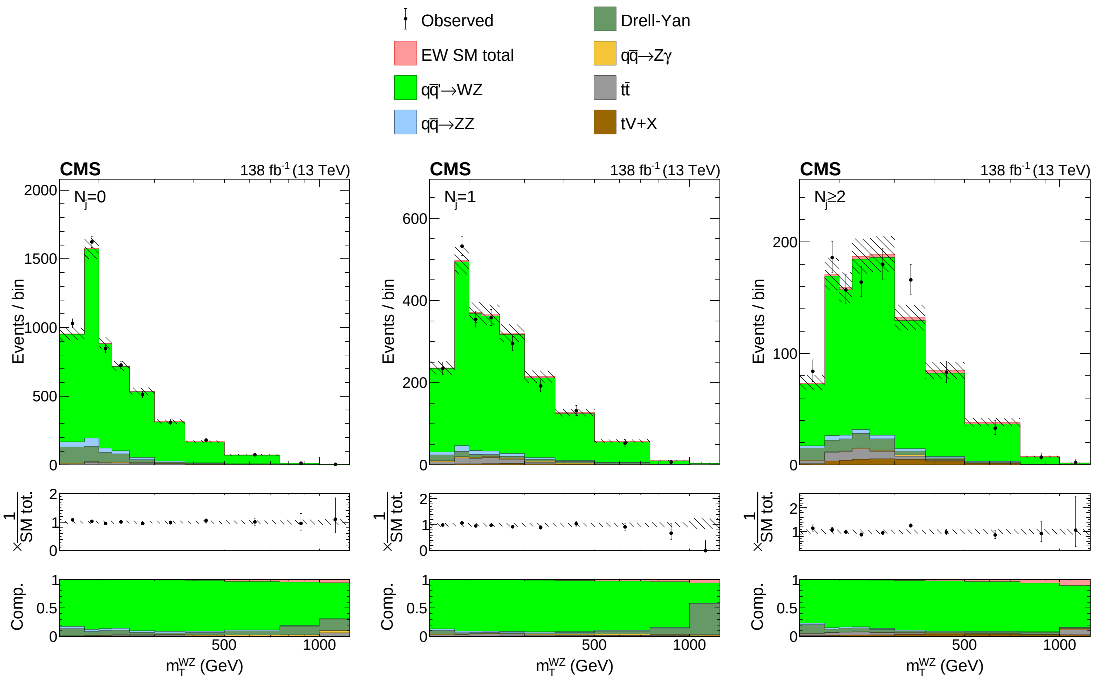

Figure S7: Postfit distributions of $m_{\mathrm{T}}^{\mathrm{WZ}}$ in the $N_{\mathrm{j}} = 0$ (left), $= 1$ (middle), and ≥ 2 (right) categories of the WZ $\to 3\ell 1\nu$ control region. The color legend for the stacked or dashed histograms is given above the plots. Postfit refers to a combined $2\ell 2\nu + 4\ell$ fit assuming SM H boson parameters. The middle pads show the ratio of the data or dashed histograms to the stacked histogram, and the lower pads show the relative contributions of each process in the stacked histogram. The rightmost bins contain the overflow.

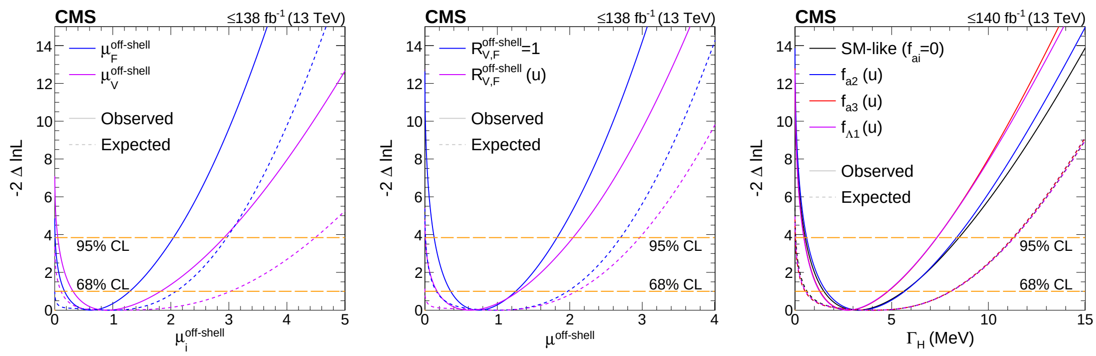

Figure S8: Observed (solid) and expected (dashed) likelihood scans for $\mu_{\mathrm{F}}^{\text{off-shell}}$ or $\mu_{\mathrm{V}}^{\text{off-shell}}$ (left), $\mu^{\text{off-shell}}$ (middle), and Γ_{H} (right). Scans for $\mu_{\mathrm{F}}^{\text{off-shell}}$ (blue) and $\mu_{\mathrm{V}}^{\text{off-shell}}$ (magenta) are obtained with the other parameter unconstrained. Those for $\mu^{\text{off-shell}}$ are shown with (blue) and without (magenta) the constraint $R_{\mathrm{V,F}}^{\text{off-shell}} = 1$. Constraints on Γ_{H} are shown with and without anomalous HVV couplings. The horizontal lines indicate the 68% ($-2\Delta\ln\mathcal{L} = 1.00$) and 95% ($-2\Delta\ln\mathcal{L} = 3.84$) CL regions. The integrated luminosity reaches up to 138 fb^{-1} when only off-shell information is used, and up to 140 fb^{-1} when on-shell 4ℓ events are included.

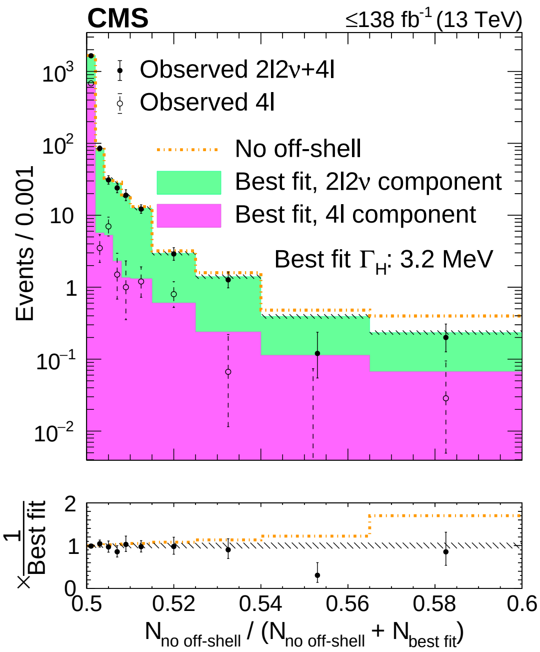

Figure S9: Distributions of ratios of the postfit number of events in each $2\ell2\nu$ and 4ℓ off-shell signal region bin. The ratios are taken after separate fits to the no off-shell ($\Gamma_{\mathrm{H}} = 0\,\mathrm{MeV}$) hypothesis ($N_{\text{no off-shell}}$) and the best overall fit ($N_{\text{best fit}}$). The stacked histograms display the predicted contributions after the best fit, and the gold dot-dashed line shows the predicted distribution of these ratios for a fit to the no off-shell ($\Gamma_{\mathrm{H}} = 0\,\mathrm{MeV}$) hypothesis. The black points represent the observed data. The first and last bins contain the overflow, and the black hashed band represents the combined postfit uncertainty on the best fit. The bottom panel displays the ratio of the various displayed hypotheses or observed data to the prediction from the best fit. The integrated luminosity reaches only up to $138\,\mathrm{fb}^{-1}$ since on-shell 4ℓ events are not displayed.

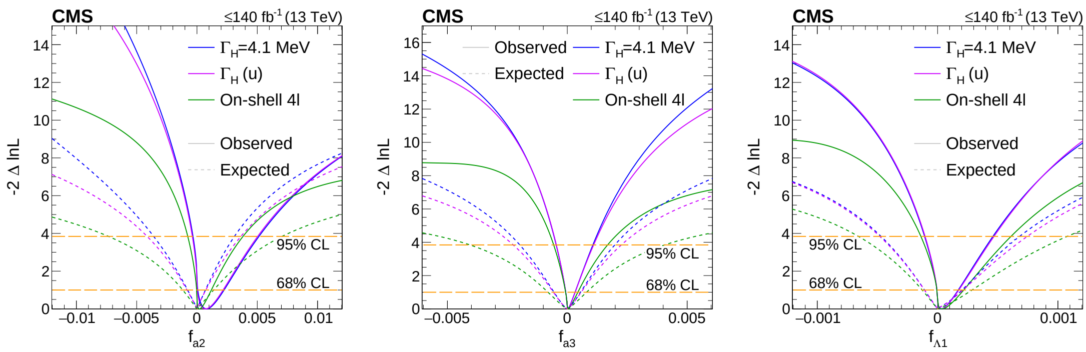

Figure S10: Likelihood scans of f_{a2} (left), f_{a3} (middle), and $f_{\Lambda1}$ (right) are shown with the constraint $\Gamma_{\mathrm{H}} = \Gamma_{\mathrm{H}}^{\mathrm{SM}} = 4.1\,\mathrm{GeV}$ (blue), Γ_{H} unconstrained (magenta), or based on on-shell 4ℓ only (green). Observed (expected) scans are shown with solid (dashed) curves. The horizontal lines indicate the 68% ($-2\Delta\ln\mathcal{L} = 1.00$) and 95% ($-2\Delta\ln\mathcal{L} = 3.84$) CL regions. The integrated luminosity reaches up to $140\,\mathrm{fb}^{-1}$ as on-shell 4ℓ events are included in the fits.

Table S1: Summary of results on Γ_H (in units of MeV) under different anomalous HVV coupling scenarios. Tests with the anomalous HVV couplings are distinguished by the denoted on-shell cross section fractions. The expected central values (not shown) are always $\Gamma_H = 4.1$ MeV. The various fit conditions are indicated in the column labeled "Cond.", where the abbreviation "(u)" indicates which f_{ai} fraction is unconstrained. The SM-like result is the same as that from the combination of all 4ℓ and $2\ell2\nu$ data sets in Table 1.

Param.	Cond.	Observed	Expected
		68% | 95% CL	68% | 95% CL
Γ_H	SM-like	$3.2^{+2.4}_{-1.7}\ \vert^{+5.3}_{-2.7}$	${}^{+4.0}_{-3.48}\ \vert^{+7.2}_{-4.065}$
Γ_H	f_{a2} (u)	$3.4^{+2.3}_{-1.8}\ \vert^{+5.0}_{-2.8}$	${}^{+3.9}_{-3.6}\ \vert^{+7.2}_{-4.085}$
Γ_H	f_{a3} (u)	$2.7^{+2.1}_{-1.4}\ \vert^{+4.6}_{-2.2}$	${}^{+3.9}_{-3.6}\ \vert^{+7.2}_{-4.085}$
Γ_H	$f_{\Lambda1}$ (u)	$2.7^{+2.1}_{-1.4}\ \vert^{+4.5}_{-2.2}$	${}^{+4.0}_{-3.6}\ \vert^{+7.2}_{-4.081}$

Table S2: Summary of the allowed 68% and 95% CL intervals for the anomalous HVV coupling parameters f_{ai}, obtained from the combined analysis of on-shell and off-shell events. Constraints are shown with either $\Gamma_H = \Gamma_H^{SM} = 4.1$ GeV required, or Γ_H left unconstrained. The designation 'b.f.' stands for the best-fit value for these parameters. The expected best-fit values are always null, so they are not quoted explicitly.

Parameter ($\times 10^5$)	Scenario	b.f.	Observed 68% | 95% CL	Expected 68% | 95% CL
f_{a2}	$\Gamma_H = \Gamma_H^{SM}$	79	[6.6, 225] | [−32, 514]	[−78, 70] | [−359, 311]
	Γ_H unconst.	72	[2.7, 216] | [−38, 503]	[−82, 73] | [−413, 364]
f_{a3}	$\Gamma_H = \Gamma_H^{SM}$	2.2	[−6.4, 32] | [−46, 107]	[−55, 55] | [−198, 198]
	Γ_H unconst.	2.4	[−6.2, 33] | [−46, 110]	[−58, 58] | [−225, 225]
$f_{\Lambda1}$	$\Gamma_H = \Gamma_H^{SM}$	2.9	[−0.62, 17] | [−11, 46]	[−11, 20] | [−47, 68]
	Γ_H unconst.	3.1	[−0.56, 18] | [−10, 47]	[−11, 21] | [−48, 75]

Acknowledgments

We congratulate our colleagues in the CERN accelerator departments for the excellent performance of the LHC and thank the technical and administrative staffs at CERN and at other CMS institutes for their contributions to the success of the CMS effort. In addition, we gratefully acknowledge the computing centers and personnel of the Worldwide LHC Computing Grid and other centers for delivering so effectively the computing infrastructure essential to our analyses. Finally, we acknowledge the enduring support for the construction and operation of the LHC, the CMS detector, and the supporting computing infrastructure provided by the following funding agencies: BMBWF and FWF (Austria); FNRS and FWO (Belgium); CNPq, CAPES, FAPERJ, FAPERGS, and FAPESP (Brazil); MES and BNSF (Bulgaria); CERN; CAS, MoST, and NSFC (China); MINCIENCIAS (Colombia); MSES and CSF (Croatia); RIF (Cyprus); SENESCYT (Ecuador); MoER, ERC PUT and ERDF (Estonia); Academy of Finland, MEC, and HIP (Finland); CEA and CNRS/IN2P3 (France); BMBF, DFG, and HGF (Germany); GSRI (Greece); NKFIA (Hungary); DAE and DST (India); IPM (Iran); SFI (Ireland); INFN (Italy); MSIP and NRF (Republic of Korea); MES (Latvia); LAS (Lithuania); MOE and UM (Malaysia); BUAP, CINVESTAV, CONACYT, LNS, SEP, and UASLP-FAI (Mexico); MOS (Montenegro); MBIE (New Zealand); PAEC (Pakistan); MSHE and NSC (Poland); FCT (Portugal); JINR (Dubna); MON, RosAtom, RAS, RFBR, and NRC KI (Russia); MESTD (Serbia); MCIN/AEI and PCTI (Spain); MOSTR (Sri Lanka); Swiss Funding Agencies (Switzerland); MST (Taipei); ThEPCenter, IPST, STAR, and NSTDA (Thailand); TUBITAK and TAEK (Turkey); NASU (Ukraine); STFC (United Kingdom); DOE and NSF (USA).

Individuals have received support from the Marie-Curie program and the European Research Council and Horizon 2020 Grant, contract Nos. 675440, 724704, 752730, 758316, 765710, 824093, 884104, and COST Action CA16108 (European Union); the Leventis Foundation; the Alfred P. Sloan Foundation; the Alexander von Humboldt Foundation; the Belgian Federal Science Policy Office; the Fonds pour la Formation à la Recherche dans l'Industrie et dans l'Agriculture (FRIA-Belgium); the Agentschap voor Innovatie door Wetenschap en Technologie (IWT-Belgium); the F.R.S.-FNRS and FWO (Belgium) under the "Excellence of Science – EOS" – be.h project n. 30820817; the Beijing Municipal Science & Technology Commission, No. Z191100007219010; the Ministry of Education, Youth and Sports (MEYS) of the Czech Republic; the Deutsche Forschungsgemeinschaft (DFG), under Germany's Excellence Strategy – EXC 2121 "Quantum Universe" – 390833306, and under project number 400140256 - GRK2497; the Lendület ("Momentum") Program and the János Bolyai Research Scholarship of the Hungarian Academy of Sciences, the New National Excellence Program ÚNKP, the NKFIA research grants 123842, 123959, 124845, 124850, 125105, 128713, 128786, and 129058 (Hungary); the Council of Science and Industrial Research, India; the Latvian Council of Science; the Ministry of Science and Higher Education and the National Science Center, contracts Opus 2014/15/B/ST2/03998 and 2015/19/B/ST2/02861 (Poland); the Fundação para a Ciência e a Tecnologia, grant CEECIND/01334/2018 (Portugal); the National Priorities Research Program by Qatar National Research Fund; the Ministry of Science and Higher Education, projects no. 0723-2020-0041 and no. FSWW-2020-0008 (Russia); MCIN/AEI/10.13039/501100011033, ERDF "a way of making Europe", and the Programa Estatal de Fomento de la Investigación Científica y Técnica de Excelencia María de Maeztu, grant MDM-2017-0765 and Programa Severo Ochoa del Principado de Asturias (Spain); the Stavros Niarchos Foundation (Greece); the Rachadapisek Sompot Fund for Postdoctoral Fellowship, Chulalongkorn University and the Chulalongkorn Academic into Its 2nd Century Project Advancement Project (Thailand); the Kavli Foundation; the Nvidia Corporation; the SuperMicro Corporation; the Welch Foundation, contract C-1845; and the Weston Havens Foundation (USA).

A The CMS Collaboration

Yerevan Physics Institute, Yerevan, Armenia
A. Tumasyan

Institut für Hochenergiephysik, Vienna, Austria
W. Adam, J.W. Andrejkovic, T. Bergauer, S. Chatterjee, K. Damanakis, M. Dragicevic, A. Escalante Del Valle, R. Frühwirth[1], M. Jeitler[1], N. Krammer, L. Lechner, D. Liko, I. Mikulec, P. Paulitsch, F.M. Pitters, J. Schieck[1], R. Schöfbeck, D. Schwarz, S. Templ, W. Waltenberger, C.-E. Wulz[1]

Institute for Nuclear Problems, Minsk, Belarus
V. Chekhovsky, A. Litomin, V. Makarenko

Universiteit Antwerpen, Antwerpen, Belgium
M.R. Darwish[2], E.A. De Wolf, T. Janssen, T. Kello[3], A. Lelek, H. Rejeb Sfar, P. Van Mechelen, S. Van Putte, N. Van Remortel

Vrije Universiteit Brussel, Brussel, Belgium
E.S. Bols, J. D'Hondt, A. De Moor, M. Delcourt, H. El Faham, S. Lowette, S. Moortgat, A. Morton, D. Müller, A.R. Sahasransu, S. Tavernier, W. Van Doninck, D. Vannerom

Université Libre de Bruxelles, Bruxelles, Belgium
D. Beghin, B. Bilin, B. Clerbaux, G. De Lentdecker, L. Favart, A.K. Kalsi, K. Lee, M. Mahdavikhorrami, I. Makarenko, S. Paredes, L. Pétré, A. Popov, N. Postiau, E. Starling, L. Thomas, M. Vanden Bemden, C. Vander Velde, P. Vanlaer

Ghent University, Ghent, Belgium
T. Cornelis, D. Dobur, J. Knolle, L. Lambrecht, G. Mestdach, M. Niedziela, C. Rendón, C. Roskas, A. Samalan, K. Skovpen, M. Tytgat, N. Van Den Bossche, B. Vermassen, L. Wezenbeek

Université Catholique de Louvain, Louvain-la-Neuve, Belgium
A. Benecke, A. Bethani, G. Bruno, F. Bury, C. Caputo, P. David, C. Delaere, I.S. Donertas, A. Giammanco, K. Jaffel, Sa. Jain, V. Lemaitre, K. Mondal, J. Prisciandaro, A. Taliercio, M. Teklishyn, T.T. Tran, P. Vischia, S. Wertz

Centro Brasileiro de Pesquisas Fisicas, Rio de Janeiro, Brazil
G.A. Alves, C. Hensel, A. Moraes, P. Rebello Teles

Universidade do Estado do Rio de Janeiro, Rio de Janeiro, Brazil
W.L. Aldá Júnior, M. Alves Gallo Pereira, M. Barroso Ferreira Filho, H. Brandao Malbouisson, W. Carvalho, J. Chinellato[4], E.M. Da Costa, G.G. Da Silveira[5], D. De Jesus Damiao, V. Dos Santos Sousa, S. Fonseca De Souza, C. Mora Herrera, K. Mota Amarilo, L. Mundim, H. Nogima, A. Santoro, S.M. Silva Do Amaral, A. Sznajder, M. Thiel, F. Torres Da Silva De Araujo[6], A. Vilela Pereira

Universidade Estadual Paulista (a), Universidade Federal do ABC (b), São Paulo, Brazil
C.A. Bernardes[5], L. Calligaris, T.R. Fernandez Perez Tomei, E.M. Gregores, D.S. Lemos, P.G. Mercadante, S.F. Novaes, Sandra S. Padula

Institute for Nuclear Research and Nuclear Energy, Bulgarian Academy of Sciences, Sofia, Bulgaria
A. Aleksandrov, G. Antchev, R. Hadjiiska, P. Iaydjiev, M. Misheva, M. Rodozov, M. Shopova,

G. Sultanov

University of Sofia, Sofia, Bulgaria
A. Dimitrov, T. Ivanov, L. Litov, B. Pavlov, P. Petkov, A. Petrov

Beihang University, Beijing, China
T. Cheng, T. Javaid[7], M. Mittal, H. Wang[3], L. Yuan

Department of Physics, Tsinghua University, Beijing, China
M. Ahmad, G. Bauer, C. Dozen[8], Z. Hu, J. Martins[9], Y. Wang, K. Yi[10,11]

Institute of High Energy Physics, Beijing, China
E. Chapon, G.M. Chen[7], H.S. Chen[7], M. Chen, F. Iemmi, A. Kapoor, D. Leggat, H. Liao, Z.-A. Liu[7], V. Milosevic, F. Monti, R. Sharma, J. Tao, J. Thomas-Wilsker, J. Wang, H. Zhang, J. Zhao

State Key Laboratory of Nuclear Physics and Technology, Peking University, Beijing, China
A. Agapitos, Y. An, Y. Ban, C. Chen, A. Levin, Q. Li, X. Lyu, Y. Mao, S.J. Qian, D. Wang, J. Xiao, H. Yang

Sun Yat-Sen University, Guangzhou, China
M. Lu, Z. You

Institute of Modern Physics and Key Laboratory of Nuclear Physics and Ion-beam Application (MOE) - Fudan University, Shanghai, China
X. Gao[3], H. Okawa, Y. Zhang

Zhejiang University, Hangzhou, China, Zhejiang, China
Z. Lin, M. Xiao

Universidad de Los Andes, Bogota, Colombia
C. Avila, A. Cabrera, C. Florez, J. Fraga

Universidad de Antioquia, Medellin, Colombia
J. Mejia Guisao, F. Ramirez, J.D. Ruiz Alvarez

University of Split, Faculty of Electrical Engineering, Mechanical Engineering and Naval Architecture, Split, Croatia
D. Giljanovic, N. Godinovic, D. Lelas, I. Puljak

University of Split, Faculty of Science, Split, Croatia
Z. Antunovic, M. Kovac, T. Sculac

Institute Rudjer Boskovic, Zagreb, Croatia
V. Brigljevic, D. Ferencek, D. Majumder, M. Roguljic, A. Starodumov[12], T. Susa

University of Cyprus, Nicosia, Cyprus
A. Attikis, K. Christoforou, G. Kole, M. Kolosova, S. Konstantinou, J. Mousa, C. Nicolaou, F. Ptochos, P.A. Razis, H. Rykaczewski, H. Saka

Charles University, Prague, Czech Republic
M. Finger[13], M. Finger Jr.[13], A. Kveton

Escuela Politecnica Nacional, Quito, Ecuador
E. Ayala

Universidad San Francisco de Quito, Quito, Ecuador
E. Carrera Jarrin

Academy of Scientific Research and Technology of the Arab Republic of Egypt, Egyptian Network of High Energy Physics, Cairo, Egypt
H. Abdalla[14], E. Salama[15,16]

Center for High Energy Physics (CHEP-FU), Fayoum University, El-Fayoum, Egypt
M.A. Mahmoud, Y. Mohammed

National Institute of Chemical Physics and Biophysics, Tallinn, Estonia
S. Bhowmik, R.K. Dewanjee, K. Ehataht, M. Kadastik, S. Nandan, C. Nielsen, J. Pata, M. Raidal, L. Tani, C. Veelken

Department of Physics, University of Helsinki, Helsinki, Finland
P. Eerola, H. Kirschenmann, K. Osterberg, M. Voutilainen

Helsinki Institute of Physics, Helsinki, Finland
S. Bharthuar, E. Brücken, F. Garcia, J. Havukainen, M.S. Kim, R. Kinnunen, T. Lampén, K. Lassila-Perini, S. Lehti, T. Lindén, M. Lotti, L. Martikainen, M. Myllymäki, J. Ott, M.m. Rantanen, H. Siikonen, E. Tuominen, J. Tuominiemi

Lappeenranta University of Technology, Lappeenranta, Finland
P. Luukka, H. Petrow, T. Tuuva

IRFU, CEA, Université Paris-Saclay, Gif-sur-Yvette, France
C. Amendola, M. Besancon, F. Couderc, M. Dejardin, D. Denegri, J.L. Faure, F. Ferri, S. Ganjour, P. Gras, G. Hamel de Monchenault, P. Jarry, B. Lenzi, J. Malcles, J. Rander, A. Rosowsky, M.Ö. Sahin, A. Savoy-Navarro[17], P. Simkina, M. Titov, G.B. Yu

Laboratoire Leprince-Ringuet, CNRS/IN2P3, Ecole Polytechnique, Institut Polytechnique de Paris, Palaiseau, France
S. Ahuja, F. Beaudette, M. Bonanomi, A. Buchot Perraguin, P. Busson, A. Cappati, C. Charlot, O. Davignon, B. Diab, G. Falmagne, B.A. Fontana Santos Alves, S. Ghosh, R. Granier de Cassagnac, A. Hakimi, I. Kucher, J. Motta, M. Nguyen, C. Ochando, P. Paganini, J. Rembser, R. Salerno, U. Sarkar, J.B. Sauvan, Y. Sirois, A. Tarabini, A. Zabi, A. Zghiche

Université de Strasbourg, CNRS, IPHC UMR 7178, Strasbourg, France
J.-L. Agram[18], J. Andrea, D. Apparu, D. Bloch, G. Bourgatte, J.-M. Brom, E.C. Chabert, C. Collard, D. Darej, J.-C. Fontaine[18], U. Goerlach, C. Grimault, A.-C. Le Bihan, E. Nibigira, P. Van Hove

Institut de Physique des 2 Infinis de Lyon (IP2I), Villeurbanne, France
E. Asilar, S. Beauceron, C. Bernet, G. Boudoul, C. Camen, A. Carle, N. Chanon, D. Contardo, P. Depasse, H. El Mamouni, J. Fay, S. Gascon, M. Gouzevitch, B. Ille, I.B. Laktineh, H. Lattaud, A. Lesauvage, M. Lethuillier, L. Mirabito, S. Perries, K. Shchablo, V. Sordini, G. Touquet, M. Vander Donckt, S. Viret

Georgian Technical University, Tbilisi, Georgia
I. Lomidze, T. Toriashvili[19], Z. Tsamalaidze[13]

RWTH Aachen University, I. Physikalisches Institut, Aachen, Germany
V. Botta, L. Feld, K. Klein, M. Lipinski, D. Meuser, A. Pauls, N. Röwert, J. Schulz, M. Teroerde

RWTH Aachen University, III. Physikalisches Institut A, Aachen, Germany
A. Dodonova, D. Eliseev, M. Erdmann, P. Fackeldey, B. Fischer, T. Hebbeker,

K. Hoepfner, F. Ivone, L. Mastrolorenzo, M. Merschmeyer, A. Meyer, G. Mocellin, S. Mondal, S. Mukherjee, D. Noll, A. Novak, A. Pozdnyakov, Y. Rath, H. Reithler, A. Schmidt, S.C. Schuler, A. Sharma, L. Vigilante, S. Wiedenbeck, S. Zaleski

RWTH Aachen University, III. Physikalisches Institut B, Aachen, Germany
C. Dziwok, G. Flügge, W. Haj Ahmad[20], O. Hlushchenko, T. Kress, A. Nowack, O. Pooth, D. Roy, A. Stahl[21], T. Ziemons, A. Zotz

Deutsches Elektronen-Synchrotron, Hamburg, Germany
H. Aarup Petersen, M. Aldaya Martin, P. Asmuss, S. Baxter, M. Bayatmakou, O. Behnke, A. Bermúdez Martínez, S. Bhattacharya, A.A. Bin Anuar, F. Blekman[22], K. Borras[23], D. Brunner, A. Campbell, A. Cardini, C. Cheng, F. Colombina, S. Consuegra Rodríguez, G. Correia Silva, M. De Silva, L. Didukh, G. Eckerlin, D. Eckstein, L.I. Estevez Banos, O. Filatov, E. Gallo[22], A. Geiser, A. Giraldi, G. Greau, A. Grohsjean, M. Guthoff, A. Jafari[24], N.Z. Jomhari, H. Jung, A. Kasem[23], M. Kasemann, H. Kaveh, C. Kleinwort, R. Kogler, D. Krücker, W. Lange, K. Lipka, W. Lohmann[25], R. Mankel, I.-A. Melzer-Pellmann, M. Mendizabal Morentin, J. Metwally, A.B. Meyer, M. Meyer, J. Mnich, A. Mussgiller, A. Nürnberg, Y. Otarid, D. Pérez Adán, D. Pitzl, A. Raspereza, B. Ribeiro Lopes, J. Rübenach, A. Saggio, A. Saibel, M. Savitskyi, M. Scham[26], V. Scheurer, S. Schnake, P. Schütze, C. Schwanenberger[22], M. Shchedrolosiev, R.E. Sosa Ricardo, D. Stafford, N. Tonon, M. Van De Klundert, F. Vazzoler, R. Walsh, D. Walter, Q. Wang, Y. Wen, K. Wichmann, L. Wiens, C. Wissing, S. Wuchterl

University of Hamburg, Hamburg, Germany
R. Aggleton, S. Albrecht, S. Bein, L. Benato, P. Connor, K. De Leo, M. Eich, K. El Morabit, F. Feindt, A. Fröhlich, C. Garbers, E. Garutti, P. Gunnellini, M. Hajheidari, J. Haller, A. Hinzmann, G. Kasieczka, R. Klanner, T. Kramer, V. Kutzner, J. Lange, T. Lange, A. Lobanov, A. Malara, C. Matthies, A. Mehta, L. Moureaux, A. Nigamova, K.J. Pena Rodriguez, M. Rieger, O. Rieger, P. Schleper, M. Schröder, J. Schwandt, J. Sonneveld, H. Stadie, G. Steinbrück, A. Tews, I. Zoi

Karlsruher Institut fuer Technologie, Karlsruhe, Germany
J. Bechtel, S. Brommer, M. Burkart, E. Butz, R. Caspart, T. Chwalek, W. De Boer[†], A. Dierlamm, A. Droll, N. Faltermann, M. Giffels, J.O. Gosewisch, A. Gottmann, F. Hartmann[21], C. Heidecker, U. Husemann, P. Keicher, R. Koppenhöfer, S. Maier, S. Mitra, Th. Müller, M. Neukum, G. Quast, K. Rabbertz, J. Rauser, D. Savoiu, M. Schnepf, D. Seith, I. Shvetsov, H.J. Simonis, R. Ulrich, J. Van Der Linden, R.F. Von Cube, M. Wassmer, M. Weber, S. Wieland, R. Wolf, S. Wozniewski, S. Wunsch

Institute of Nuclear and Particle Physics (INPP), NCSR Demokritos, Aghia Paraskevi, Greece
G. Anagnostou, G. Daskalakis, A. Kyriakis, D. Loukas, A. Stakia

National and Kapodistrian University of Athens, Athens, Greece
M. Diamantopoulou, D. Karasavvas, P. Kontaxakis, C.K. Koraka, A. Manousakis-Katsikakis, A. Panagiotou, I. Papavergou, N. Saoulidou, K. Theofilatos, E. Tziaferi, K. Vellidis, E. Vourliotis

National Technical University of Athens, Athens, Greece
G. Bakas, K. Kousouris, I. Papakrivopoulos, G. Tsipolitis, A. Zacharopoulou

University of Ioánnina, Ioánnina, Greece

K. Adamidis, I. Bestintzanos, I. Evangelou, C. Foudas, P. Gianneios, P. Katsoulis, P. Kokkas, N. Manthos, I. Papadopoulos, J. Strologas

MTA-ELTE Lendület CMS Particle and Nuclear Physics Group, Eötvös Loránd University, Budapest, Hungary
M. Csanad, K. Farkas, M.M.A. Gadallah[27], S. Lökös[28], P. Major, K. Mandal, G. Pasztor, A.J. Rádl, O. Surányi, G.I. Veres

Wigner Research Centre for Physics, Budapest, Hungary
M. Bartók[29], G. Bencze, C. Hajdu, D. Horvath[30,31], F. Sikler, V. Veszpremi

Institute of Nuclear Research ATOMKI, Debrecen, Hungary
S. Czellar, D. Fasanella, F. Fienga, J. Karancsi[29], J. Molnar, Z. Szillasi, D. Teyssier

Institute of Physics, University of Debrecen, Debrecen, Hungary
P. Raics, Z.L. Trocsanyi[32], B. Ujvari[33]

Karoly Robert Campus, MATE Institute of Technology, Gyongyos, Hungary
T. Csorgo[34], F. Nemes[34], T. Novak

National Institute of Science Education and Research, HBNI, Bhubaneswar, India
S. Bahinipati[35], C. Kar, P. Mal, T. Mishra, V.K. Muraleedharan Nair Bindhu[36], A. Nayak[36], P. Saha, N. Sur, S.K. Swain, D. Vats[36]

Panjab University, Chandigarh, India
S. Bansal, S.B. Beri, V. Bhatnagar, G. Chaudhary, S. Chauhan, N. Dhingra[37], R. Gupta, A. Kaur, H. Kaur, M. Kaur, P. Kumari, M. Meena, K. Sandeep, J.B. Singh[38], A.K. Virdi

University of Delhi, Delhi, India
A. Ahmed, A. Bhardwaj, B.C. Choudhary, M. Gola, S. Keshri, A. Kumar, M. Naimuddin, P. Priyanka, K. Ranjan, S. Saumya, A. Shah

Saha Institute of Nuclear Physics, HBNI, Kolkata, India
M. Bharti[39], R. Bhattacharya, S. Bhattacharya, D. Bhowmik, S. Dutta, S. Dutta, B. Gomber[40], M. Maity[41], P. Palit, P.K. Rout, G. Saha, B. Sahu, S. Sarkar, M. Sharan

Indian Institute of Technology Madras, Madras, India
P.K. Behera, S.C. Behera, P. Kalbhor, J.R. Komaragiri[42], D. Kumar[42], A. Muhammad, L. Panwar[42], R. Pradhan, P.R. Pujahari, A. Sharma, A.K. Sikdar, P.C. Tiwari[42]

Bhabha Atomic Research Centre, Mumbai, India
K. Naskar[43]

Tata Institute of Fundamental Research-A, Mumbai, India
T. Aziz, S. Dugad, M. Kumar, G.B. Mohanty

Tata Institute of Fundamental Research-B, Mumbai, India
S. Banerjee, R. Chudasama, M. Guchait, S. Karmakar, S. Kumar, G. Majumder, K. Mazumdar, S. Mukherjee

Indian Institute of Science Education and Research (IISER), Pune, India
A. Alpana, S. Dube, B. Kansal, A. Laha, S. Pandey, A. Rastogi, S. Sharma

Isfahan University of Technology, Isfahan, Iran
H. Bakhshiansohi[44,45], E. Khazaie[45], M. Zeinali[46]

Institute for Research in Fundamental Sciences (IPM), Tehran, Iran
S. Chenarani[47], S.M. Etesami, M. Khakzad, M. Mohammadi Najafabadi

University College Dublin, Dublin, Ireland
M. Grunewald

INFN Sezione di Bari [a], Bari, Italy, Università di Bari [b], Bari, Italy, Politecnico di Bari [c], Bari, Italy
M. Abbrescia[a,b], R. Aly[a,b,48], C. Aruta[a,b], A. Colaleo[a], D. Creanza[a,c], N. De Filippis[a,c], M. De Palma[a,b], A. Di Florio[a,b], A. Di Pilato[a,b], W. Elmetenawee[a,b], F. Errico[a,b], L. Fiore[a], G. Iaselli[a,c], M. Ince[a,b], S. Lezki[a,b], G. Maggi[a,c], M. Maggi[a], I. Margjeka[a,b], V. Mastrapasqua[a,b], S. My[a,b], S. Nuzzo[a,b], A. Pellecchia[a,b], A. Pompili[a,b], G. Pugliese[a,c], D. Ramos[a], A. Ranieri[a], G. Selvaggi[a,b], L. Silvestris[a], F.M. Simone[a,b], Ü. Sözbilir[a], R. Venditti[a], P. Verwilligen[a]

INFN Sezione di Bologna [a], Bologna, Italy, Università di Bologna [b], Bologna, Italy
G. Abbiendi[a], C. Battilana[a,b], D. Bonacorsi[a,b], L. Borgonovi[a], L. Brigliadori[a], R. Campanini[a,b], P. Capiluppi[a,b], A. Castro[a,b], F.R. Cavallo[a], C. Ciocca[a], M. Cuffiani[a,b], G.M. Dallavalle[a], T. Diotalevi[a,b], F. Fabbri[a], A. Fanfani[a,b], P. Giacomelli[a], L. Giommi[a,b], C. Grandi[a], L. Guiducci[a,b], S. Lo Meo[a,49], L. Lunerti[a,b], S. Marcellini[a], G. Masetti[a], F.L. Navarria[a,b], A. Perrotta[a], F. Primavera[a,b], A.M. Rossi[a,b], T. Rovelli[a,b], G.P. Siroli[a,b]

INFN Sezione di Catania [a], Catania, Italy, Università di Catania [b], Catania, Italy
S. Albergo[a,b,50], S. Costa[a,b,50], A. Di Mattia[a], R. Potenza[a,b], A. Tricomi[a,b,50], C. Tuve[a,b]

INFN Sezione di Firenze [a], Firenze, Italy, Università di Firenze [b], Firenze, Italy
G. Barbagli[a], A. Cassese[a], R. Ceccarelli[a,b], V. Ciulli[a,b], C. Civinini[a], R. D'Alessandro[a,b], E. Focardi[a,b], G. Latino[a,b], P. Lenzi[a,b], M. Lizzo[a,b], M. Meschini[a], S. Paoletti[a], R. Seidita[a,b], G. Sguazzoni[a], L. Viliani[a]

INFN Laboratori Nazionali di Frascati, Frascati, Italy
L. Benussi, S. Bianco, D. Piccolo

INFN Sezione di Genova [a], Genova, Italy, Università di Genova [b], Genova, Italy
M. Bozzo[a,b], F. Ferro[a], R. Mulargia[a], E. Robutti[a], S. Tosi[a,b]

INFN Sezione di Milano-Bicocca [a], Milano, Italy, Università di Milano-Bicocca [b], Milano, Italy
A. Benaglia[a], G. Boldrini, F. Brivio[a,b], F. Cetorelli[a,b], F. De Guio[a,b], M.E. Dinardo[a,b], P. Dini[a], S. Gennai[a], A. Ghezzi[a,b], P. Govoni[a,b], L. Guzzi[a,b], M.T. Lucchini[a,b], M. Malberti[a], S. Malvezzi[a], A. Massironi[a], D. Menasce[a], L. Moroni[a], M. Paganoni[a,b], D. Pedrini[a], B.S. Pinolini, S. Ragazzi[a,b], N. Redaelli[a], T. Tabarelli de Fatis[a,b], D. Valsecchi[a,b,21], D. Zuolo[a,b]

INFN Sezione di Napoli [a], Napoli, Italy, Università di Napoli 'Federico II' [b], Napoli, Italy, Università della Basilicata [c], Potenza, Italy, Università G. Marconi [d], Roma, Italy
S. Buontempo[a], F. Carnevali[a,b], N. Cavallo[a,c], A. De Iorio[a,b], F. Fabozzi[a,c], A.O.M. Iorio[a,b], L. Lista[a,b,51], S. Meola[a,d,21], P. Paolucci[a,21], B. Rossi[a], C. Sciacca[a,b]

INFN Sezione di Padova [a], Padova, Italy, Università di Padova [b], Padova, Italy, Università di Trento [c], Trento, Italy

P. Azzi[a], N. Bacchetta[a], D. Bisello[a,b], P. Bortignon[a], A. Bragagnolo[a,b], R. Carlin[a,b], P. Checchia[a], T. Dorigo[a], U. Dosselli[a], F. Gasparini[a,b], U. Gasparini[a,b], G. Grosso, L. Layer[a,52], E. Lusiani, M. Margoni[a,b], F. Marini, A.T. Meneguzzo[a,b], J. Pazzini[a,b], P. Ronchese[a,b], R. Rossin[a,b], F. Simonetto[a,b], G. Strong[a], M. Tosi[a,b], H. Yarar[a,b], M. Zanetti[a,b], P. Zotto[a,b], A. Zucchetta[a,b], G. Zumerle[a,b]

INFN Sezione di Pavia [a], Pavia, Italy, Università di Pavia [b], Pavia, Italy
C. Aimè[a,b], A. Braghieri[a], S. Calzaferri[a,b], D. Fiorina[a,b], P. Montagna[a,b], S.P. Ratti[a,b], V. Re[a], C. Riccardi[a,b], P. Salvini[a], I. Vai[a], P. Vitulo[a,b]

INFN Sezione di Perugia [a], Perugia, Italy, Università di Perugia [b], Perugia, Italy
P. Asenov[a,53], G.M. Bilei[a], D. Ciangottini[a,b], L. Fanò[a,b], M. Magherini[b], G. Mantovani[a,b], V. Mariani[a,b], M. Menichelli[a], F. Moscatelli[a,53], A. Piccinelli[a,b], M. Presilla[a,b], A. Rossi[a,b], A. Santocchia[a,b], D. Spiga[a], T. Tedeschi[a,b]

INFN Sezione di Pisa [a], Pisa, Italy, Università di Pisa [b], Pisa, Italy, Scuola Normale Superiore di Pisa [c], Pisa, Italy, Università di Siena [d], Siena, Italy
P. Azzurri[a], G. Bagliesi[a], V. Bertacchi[a,c], L. Bianchini[a], T. Boccali[a], E. Bossini[a,b], R. Castaldi[a], M.A. Ciocci[a,b], V. D'Amante[a,d], R. Dell'Orso[a], M.R. Di Domenico[a,d], S. Donato[a], A. Giassi[a], F. Ligabue[a,c], E. Manca[a,c], G. Mandorli[a,c], D. Matos Figueiredo, A. Messineo[a,b], M. Musich[a], F. Palla[a], S. Parolia[a,b], G. Ramirez-Sanchez[a,c], A. Rizzi[a,b], G. Rolandi[a,c], S. Roy Chowdhury[a,c], A. Scribano[a], N. Shafiei[a,b], P. Spagnolo[a], R. Tenchini[a], G. Tonelli[a,b], N. Turini[a,d], A. Venturi[a], P.G. Verdini[a]

INFN Sezione di Roma [a], Rome, Italy, Sapienza Università di Roma [b], Rome, Italy
P. Barria[a], M. Campana[a,b], F. Cavallari[a], D. Del Re[a,b], E. Di Marco[a], M. Diemoz[a], E. Longo[a,b], P. Meridiani[a], G. Organtini[a,b], F. Pandolfi[a], R. Paramatti[a,b], C. Quaranta[a,b], S. Rahatlou[a,b], C. Rovelli[a], F. Santanastasio[a,b], L. Soffi[a], R. Tramontano[a,b]

INFN Sezione di Torino [a], Torino, Italy, Università di Torino [b], Torino, Italy, Università del Piemonte Orientale [c], Novara, Italy
N. Amapane[a,b], R. Arcidiacono[a,c], S. Argiro[a,b], M. Arneodo[a,c], N. Bartosik[a], R. Bellan[a,b], A. Bellora[a,b], J. Berenguer Antequera[a,b], C. Biino[a], N. Cartiglia[a], M. Costa[a,b], R. Covarelli[a,b], N. Demaria[a], M. Grippo[a,b], B. Kiani[a,b], F. Legger[a], C. Mariotti[a], S. Maselli[a], A. Mecca[a,b], E. Migliore[a,b], E. Monteil[a,b], M. Monteno[a], M.M. Obertino[a,b], G. Ortona[a], L. Pacher[a,b], N. Pastrone[a], M. Pelliccioni[a], M. Ruspa[a,c], K. Shchelina[a], F. Siviero[a,b], V. Sola[a], A. Solano[a,b], D. Soldi[a,b], A. Staiano[a], M. Tornago[a,b], D. Trocino[a], G. Umoret[a,b], A. Vagnerini[a,b]

INFN Sezione di Trieste [a], Trieste, Italy, Università di Trieste [b], Trieste, Italy
S. Belforte[a], V. Candelise[a,b], M. Casarsa[a], F. Cossutti[a], A. Da Rold[a,b], G. Della Ricca[a,b], G. Sorrentino[a,b]

Kyungpook National University, Daegu, Korea
S. Dogra, C. Huh, B. Kim, D.H. Kim, G.N. Kim, J. Kim, J. Lee, S.W. Lee, C.S. Moon, Y.D. Oh, S.I. Pak, S. Sekmen, Y.C. Yang

Chonnam National University, Institute for Universe and Elementary Particles, Kwangju, Korea
H. Kim, D.H. Moon

Hanyang University, Seoul, Korea

B. Francois, T.J. Kim, J. Park

Korea University, Seoul, Korea
S. Cho, S. Choi, B. Hong, K. Lee, K.S. Lee, J. Lim, J. Park, S.K. Park, J. Yoo

Kyung Hee University, Department of Physics, Seoul, Republic of Korea, Seoul, Korea
J. Goh, A. Gurtu

Sejong University, Seoul, Korea
H.S. Kim, Y. Kim

Seoul National University, Seoul, Korea
J. Almond, J.H. Bhyun, J. Choi, S. Jeon, J. Kim, J.S. Kim, S. Ko, H. Kwon, H. Lee, S. Lee, B.H. Oh, M. Oh, S.B. Oh, H. Seo, U.K. Yang, I. Yoon

University of Seoul, Seoul, Korea
W. Jang, D.Y. Kang, Y. Kang, S. Kim, B. Ko, J.S.H. Lee, Y. Lee, J.A. Merlin, I.C. Park, Y. Roh, M.S. Ryu, D. Song, I.J. Watson, S. Yang

Yonsei University, Department of Physics, Seoul, Korea
S. Ha, H.D. Yoo

Sungkyunkwan University, Suwon, Korea
M. Choi, H. Lee, Y. Lee, I. Yu

College of Engineering and Technology, American University of the Middle East (AUM), Egaila, Kuwait, Dasman, Kuwait
T. Beyrouthy, Y. Maghrbi

Riga Technical University, Riga, Latvia
K. Dreimanis, V. Veckalns[54]

Vilnius University, Vilnius, Lithuania
M. Ambrozas, A. Carvalho Antunes De Oliveira, A. Juodagalvis, A. Rinkevicius, G. Tamulaitis

National Centre for Particle Physics, Universiti Malaya, Kuala Lumpur, Malaysia
N. Bin Norjoharuddeen, S.Y. Hoh[55], Z. Zolkapli

Universidad de Sonora (UNISON), Hermosillo, Mexico
J.F. Benitez, A. Castaneda Hernandez, H.A. Encinas Acosta, L.G. Gallegos Maríñez, M. León Coello, J.A. Murillo Quijada, A. Sehrawat, L. Valencia Palomo

Centro de Investigacion y de Estudios Avanzados del IPN, Mexico City, Mexico
G. Ayala, H. Castilla-Valdez, E. De La Cruz-Burelo, I. Heredia-De La Cruz[56], R. Lopez-Fernandez, C.A. Mondragon Herrera, D.A. Perez Navarro, R. Reyes-Almanza, A. Sánchez Hernández

Universidad Iberoamericana, Mexico City, Mexico
S. Carrillo Moreno, C. Oropeza Barrera, F. Vazquez Valencia

Benemerita Universidad Autonoma de Puebla, Puebla, Mexico
I. Pedraza, H.A. Salazar Ibarguen, C. Uribe Estrada

University of Montenegro, Podgorica, Montenegro
I. Bubanja, J. Mijuskovic[57], N. Raicevic

University of Auckland, Auckland, New Zealand

D. Krofcheck

University of Canterbury, Christchurch, New Zealand
P.H. Butler

National Centre for Physics, Quaid-I-Azam University, Islamabad, Pakistan
A. Ahmad, M.I. Asghar, A. Awais, M.I.M. Awan, M. Gul, H.R. Hoorani, W.A. Khan, M.A. Shah, M. Shoaib, M. Waqas

AGH University of Science and Technology Faculty of Computer Science, Electronics and Telecommunications, Krakow, Poland
V. Avati, L. Grzanka, M. Malawski

National Centre for Nuclear Research, Swierk, Poland
H. Bialkowska, M. Bluj, B. Boimska, M. Górski, M. Kazana, M. Szleper, P. Zalewski

Institute of Experimental Physics, Faculty of Physics, University of Warsaw, Warsaw, Poland
K. Bunkowski, K. Doroba, A. Kalinowski, M. Konecki, J. Krolikowski

Laboratório de Instrumentação e Física Experimental de Partículas, Lisboa, Portugal
M. Araujo, P. Bargassa, D. Bastos, A. Boletti, P. Faccioli, M. Gallinaro, J. Hollar, N. Leonardo, T. Niknejad, M. Pisano, J. Seixas, O. Toldaiev, J. Varela

Joint Institute for Nuclear Research, Dubna, Russia
S. Afanasiev, D. Budkouski, I. Golutvin, I. Gorbunov, V. Karjavine, V. Korenkov, A. Lanev, A. Malakhov, V. Matveev[58,59], V. Palichik, V. Perelygin, M. Savina, V. Shalaev, S. Shmatov, S. Shulha, V. Smirnov, O. Teryaev, N. Voytishin, B.S. Yuldashev[60], A. Zarubin, I. Zhizhin

Petersburg Nuclear Physics Institute, Gatchina (St. Petersburg), Russia
G. Gavrilov, V. Golovtcov, Y. Ivanov, V. Kim[61], E. Kuznetsova[62], V. Murzin, V. Oreshkin, I. Smirnov, D. Sosnov, V. Sulimov, L. Uvarov, S. Volkov, A. Vorobyev

Institute for Nuclear Research, Moscow, Russia
Yu. Andreev, A. Dermenev, S. Gninenko, N. Golubev, A. Karneyeu, D. Kirpichnikov, M. Kirsanov, N. Krasnikov, A. Pashenkov, G. Pivovarov, A. Toropin

Moscow Institute of Physics and Technology, Moscow, Russia
T. Aushev

National Research Center 'Kurchatov Institute', Moscow, Russia
V. Epshteyn, V. Gavrilov, N. Lychkovskaya, A. Nikitenko[63], V. Popov, A. Stepennov, M. Toms, E. Vlasov, A. Zhokin

National Research Nuclear University 'Moscow Engineering Physics Institute' (MEPhI), Moscow, Russia
O. Bychkova, R. Chistov[64], M. Danilov[64], A. Oskin, P. Parygin, S. Polikarpov[64]

P.N. Lebedev Physical Institute, Moscow, Russia
V. Andreev, M. Azarkin, I. Dremin, M. Kirakosyan, A. Terkulov

Skobeltsyn Institute of Nuclear Physics, Lomonosov Moscow State University, Moscow, Russia
A. Belyaev, E. Boos, V. Bunichev, M. Dubinin[65], L. Dudko, A. Ershov, V. Klyukhin, O. Kodolova, I. Lokhtin, S. Obraztsov, M. Perfilov, S. Petrushanko, V. Savrin

Novosibirsk State University (NSU), Novosibirsk, Russia
V. Blinov[66], T. Dimova[66], L. Kardapoltsev[66], A. Kozyrev[66], I. Ovtin[66], O. Radchenko[66],

Y. Skovpen[66]

Institute for High Energy Physics of National Research Centre 'Kurchatov Institute', Protvino, Russia
I. Azhgirey, I. Bayshev, D. Elumakhov, V. Kachanov, D. Konstantinov, P. Mandrik, V. Petrov, R. Ryutin, S. Slabospitskii, A. Sobol, S. Troshin, N. Tyurin, A. Uzunian, A. Volkov

National Research Tomsk Polytechnic University, Tomsk, Russia
A. Babaev, V. Okhotnikov

Tomsk State University, Tomsk, Russia
V. Borshch, V. Ivanchenko, E. Tcherniaev

University of Belgrade: Faculty of Physics and VINCA Institute of Nuclear Sciences, Belgrade, Serbia
P. Adzic[67], M. Dordevic, P. Milenovic, J. Milosevic

Centro de Investigaciones Energéticas Medioambientales y Tecnológicas (CIEMAT), Madrid, Spain
M. Aguilar-Benitez, J. Alcaraz Maestre, A. Álvarez Fernández, I. Bachiller, M. Barrio Luna, Cristina F. Bedoya, C.A. Carrillo Montoya, M. Cepeda, M. Cerrada, N. Colino, B. De La Cruz, A. Delgado Peris, J.P. Fernández Ramos, J. Flix, M.C. Fouz, O. Gonzalez Lopez, S. Goy Lopez, J.M. Hernandez, M.I. Josa, J. León Holgado, D. Moran, Á. Navarro Tobar, C. Perez Dengra, A. Pérez-Calero Yzquierdo, J. Puerta Pelayo, I. Redondo, L. Romero, S. Sánchez Navas, L. Urda Gómez, C. Willmott

Universidad Autónoma de Madrid, Madrid, Spain
J.F. de Trocóniz

Universidad de Oviedo, Instituto Universitario de Ciencias y Tecnologías Espaciales de Asturias (ICTEA), Oviedo, Spain
B. Alvarez Gonzalez, J. Cuevas, J. Fernandez Menendez, S. Folgueras, I. Gonzalez Caballero, J.R. González Fernández, E. Palencia Cortezon, C. Ramón Álvarez, V. Rodríguez Bouza, A. Soto Rodríguez, A. Trapote, N. Trevisani, C. Vico Villalba

Instituto de Física de Cantabria (IFCA), CSIC-Universidad de Cantabria, Santander, Spain
J.A. Brochero Cifuentes, I.J. Cabrillo, A. Calderon, J. Duarte Campderros, M. Fernandez, C. Fernandez Madrazo, P.J. Fernández Manteca, A. García Alonso, G. Gomez, C. Martinez Rivero, P. Martinez Ruiz del Arbol, F. Matorras, P. Matorras Cuevas, J. Piedra Gomez, C. Prieels, A. Ruiz-Jimeno, L. Scodellaro, I. Vila, J.M. Vizan Garcia

University of Colombo, Colombo, Sri Lanka
M.K. Jayananda, B. Kailasapathy[68], D.U.J. Sonnadara, D.D.C. Wickramarathna

University of Ruhuna, Department of Physics, Matara, Sri Lanka
W.G.D. Dharmaratna, K. Liyanage, N. Perera, N. Wickramage

CERN, European Organization for Nuclear Research, Geneva, Switzerland
T.K. Aarrestad, D. Abbaneo, J. Alimena, E. Auffray, G. Auzinger, J. Baechler, P. Baillon[†], D. Barney, J. Bendavid, M. Bianco, A. Bocci, C. Caillol, T. Camporesi, M. Capeans Garrido, G. Cerminara, N. Chernyavskaya, S.S. Chhibra, S. Choudhury, M. Cipriani, L. Cristella, D. d'Enterria, A. Dabrowski, A. David, A. De Roeck, M.M. Defranchis, M. Deile, M. Dobson, M. Dünser, N. Dupont, A. Elliott-Peisert, F. Fallavollita[69], A. Florent, L. Forthomme, G. Franzoni, W. Funk, S. Ghosh, S. Giani, D. Gigi, K. Gill, F. Glege, L. Gouskos, E. Govorkova, M. Haranko, J. Hegeman,

V. Innocente, T. James, P. Janot, J. Kaspar, J. Kieseler, M. Komm, N. Kratochwil, C. Lange, S. Laurila, P. Lecoq, A. Lintuluoto, C. Lourenço, B. Maier, L. Malgeri, S. Mallios, M. Mannelli, A.C. Marini, F. Meijers, S. Mersi, E. Meschi, F. Moortgat, M. Mulders, S. Orfanelli, L. Orsini, F. Pantaleo, E. Perez, M. Peruzzi, A. Petrilli, G. Petrucciani, A. Pfeiffer, M. Pierini, D. Piparo, M. Pitt, H. Qu, T. Quast, D. Rabady, A. Racz, G. Reales Gutiérrez, M. Rovere, H. Sakulin, J. Salfeld-Nebgen, S. Scarfi, C. Schwick, M. Selvaggi, A. Sharma, P. Silva, W. Snoeys, P. Sphicas[70], S. Summers, K. Tatar, V.R. Tavolaro, D. Treille, P. Tropea, A. Tsirou, J. Wanczyk[71], K.A. Wozniak, W.D. Zeuner

Paul Scherrer Institut, Villigen, Switzerland
L. Caminada[72], A. Ebrahimi, W. Erdmann, R. Horisberger, Q. Ingram, H.C. Kaestli, D. Kotlinski, U. Langenegger, M. Missiroli[72], L. Noehte[72], T. Rohe

ETH Zurich - Institute for Particle Physics and Astrophysics (IPA), Zurich, Switzerland
K. Androsov[71], M. Backhaus, P. Berger, A. Calandri, A. De Cosa, G. Dissertori, M. Dittmar, M. Donegà, C. Dorfer, F. Eble, K. Gedia, F. Glessgen, T.A. Gómez Espinosa, C. Grab, D. Hits, W. Lustermann, A.-M. Lyon, R.A. Manzoni, L. Marchese, C. Martin Perez, M.T. Meinhard, F. Nessi-Tedaldi, J. Niedziela, F. Pauss, V. Perovic, S. Pigazzini, M.G. Ratti, M. Reichmann, C. Reissel, T. Reitenspiess, B. Ristic, D. Ruini, D.A. Sanz Becerra, V. Stampf, J. Steggemann[71], R. Wallny

Universität Zürich, Zurich, Switzerland
C. Amsler[73], P. Bärtschi, C. Botta, D. Brzhechko, M.F. Canelli, K. Cormier, A. De Wit, R. Del Burgo, J.K. Heikkilä, M. Huwiler, W. Jin, A. Jofrehei, B. Kilminster, S. Leontsinis, S.P. Liechti, A. Macchiolo, P. Meiring, V.M. Mikuni, U. Molinatti, I. Neutelings, A. Reimers, P. Robmann, S. Sanchez Cruz, K. Schweiger, M. Senger, Y. Takahashi

National Central University, Chung-Li, Taiwan
C. Adloff[74], C.M. Kuo, W. Lin, A. Roy, T. Sarkar[41], S.S. Yu

National Taiwan University (NTU), Taipei, Taiwan
L. Ceard, Y. Chao, K.F. Chen, P.H. Chen, P.s. Chen, H. Cheng, W.-S. Hou, Y.y. Li, R.-S. Lu, E. Paganis, A. Psallidas, A. Steen, H.y. Wu, E. Yazgan, P.r. Yu

Chulalongkorn University, Faculty of Science, Department of Physics, Bangkok, Thailand
B. Asavapibhop, C. Asawatangtrakuldee, N. Srimanobhas

Çukurova University, Physics Department, Science and Art Faculty, Adana, Turkey
F. Boran, S. Damarseckin[75], Z.S. Demiroglu, F. Dolek, I. Dumanoglu[76], E. Eskut, Y. Guler[77], E. Gurpinar Guler[77], C. Isik, O. Kara, A. Kayis Topaksu, U. Kiminsu, G. Onengut, K. Ozdemir[78], A. Polatoz, A.E. Simsek, B. Tali[79], U.G. Tok, S. Turkcapar, I.S. Zorbakir

Middle East Technical University, Physics Department, Ankara, Turkey
G. Karapinar, K. Ocalan[80], M. Yalvac[81]

Bogazici University, Istanbul, Turkey
B. Akgun, I.O. Atakisi, E. Gulmez, M. Kaya[82], O. Kaya[83], Ö. Özçelik, S. Tekten[84], E.A. Yetkin[85]

Istanbul Technical University, Istanbul, Turkey
A. Cakir, K. Cankocak[76], Y. Komurcu, S. Sen[86]

Istanbul University, Istanbul, Turkey
S. Cerci[79], I. Hos[87], B. Isildak[88], B. Kaynak, S. Ozkorucuklu, H. Sert, C. Simsek, D. Sunar Cerci[79], C. Zorbilmez

Institute for Scintillation Materials of National Academy of Science of Ukraine, Kharkov, Ukraine
B. Grynyov

National Scientific Center, Kharkov Institute of Physics and Technology, Kharkov, Ukraine
L. Levchuk

University of Bristol, Bristol, United Kingdom
D. Anthony, E. Bhal, S. Bologna, J.J. Brooke, A. Bundock, E. Clement, D. Cussans, H. Flacher, M. Glowacki, J. Goldstein, G.P. Heath, H.F. Heath, L. Kreczko, B. Krikler, S. Paramesvaran, S. Seif El Nasr-Storey, V.J. Smith, N. Stylianou[89], K. Walkingshaw Pass, R. White

Rutherford Appleton Laboratory, Didcot, United Kingdom
K.W. Bell, A. Belyaev[90], C. Brew, R.M. Brown, D.J.A. Cockerill, C. Cooke, K.V. Ellis, K. Harder, S. Harper, M.-L. Holmberg[91], J. Linacre, K. Manolopoulos, D.M. Newbold, E. Olaiya, D. Petyt, T. Reis, T. Schuh, C.H. Shepherd-Themistocleous, I.R. Tomalin, T. Williams

Imperial College, London, United Kingdom
R. Bainbridge, P. Bloch, S. Bonomally, J. Borg, S. Breeze, O. Buchmuller, V. Cepaitis, G.S. Chahal[92], D. Colling, P. Dauncey, G. Davies, M. Della Negra, S. Fayer, G. Fedi, G. Hall, M.H. Hassanshahi, G. Iles, J. Langford, L. Lyons, A.-M. Magnan, S. Malik, A. Martelli, D.G. Monk, J. Nash[93], M. Pesaresi, B.C. Radburn-Smith, D.M. Raymond, A. Richards, A. Rose, E. Scott, C. Seez, A. Shtipliyski, A. Tapper, K. Uchida, T. Virdee[21], M. Vojinovic, N. Wardle, S.N. Webb, D. Winterbottom

Brunel University, Uxbridge, United Kingdom
K. Coldham, J.E. Cole, A. Khan, P. Kyberd, I.D. Reid, L. Teodorescu, S. Zahid

Baylor University, Waco, Texas, USA
S. Abdullin, A. Brinkerhoff, B. Caraway, J. Dittmann, K. Hatakeyama, A.R. Kanuganti, B. McMaster, M. Saunders, S. Sawant, C. Sutantawibul, J. Wilson

Catholic University of America, Washington, DC, USA
R. Bartek, A. Dominguez, R. Uniyal, A.M. Vargas Hernandez

The University of Alabama, Tuscaloosa, Alabama, USA
A. Buccilli, S.I. Cooper, D. Di Croce, S.V. Gleyzer, C. Henderson, C.U. Perez, P. Rumerio[94], C. West

Boston University, Boston, Massachusetts, USA
A. Akpinar, A. Albert, D. Arcaro, C. Cosby, Z. Demiragli, C. Erice, E. Fontanesi, D. Gastler, S. May, J. Rohlf, K. Salyer, D. Sperka, D. Spitzbart, I. Suarez, A. Tsatsos, S. Yuan, D. Zou

Brown University, Providence, Rhode Island, USA
G. Benelli, B. Burkle, X. Coubez[23], D. Cutts, M. Hadley, U. Heintz, J.M. Hogan[95], T. Kwon, G. Landsberg, K.T. Lau, D. Li, M. Lukasik, J. Luo, M. Narain, N. Pervan, S. Sagir[96], F. Simpson, E. Usai, W.Y. Wong, X. Yan, D. Yu, W. Zhang

University of California, Davis, Davis, California, USA
J. Bonilla, C. Brainerd, R. Breedon, M. Calderon De La Barca Sanchez, M. Chertok, J. Conway, P.T. Cox, R. Erbacher, G. Haza, F. Jensen, O. Kukral, R. Lander, M. Mulhearn, D. Pellett, B. Regnery, D. Taylor, Y. Yao, F. Zhang

University of California, Los Angeles, California, USA
M. Bachtis, R. Cousins, A. Datta, D. Hamilton, J. Hauser, M. Ignatenko, M.A. Iqbal, T. Lam, W.A. Nash, S. Regnard, D. Saltzberg, B. Stone, V. Valuev

University of California, Riverside, Riverside, California, USA
Y. Chen, R. Clare, J.W. Gary, M. Gordon, G. Hanson, G. Karapostoli, O.R. Long, N. Manganelli, W. Si, S. Wimpenny, Y. Zhang

University of California, San Diego, La Jolla, California, USA
J.G. Branson, P. Chang, S. Cittolin, S. Cooperstein, D. Diaz, J. Duarte, R. Gerosa, L. Giannini, J. Guiang, R. Kansal, V. Krutelyov, R. Lee, J. Letts, M. Masciovecchio, F. Mokhtar, M. Pieri, B.V. Sathia Narayanan, V. Sharma, M. Tadel, F. Würthwein, Y. Xiang, A. Yagil

University of California, Santa Barbara - Department of Physics, Santa Barbara, California, USA
N. Amin, C. Campagnari, M. Citron, G. Collura, A. Dorsett, V. Dutta, J. Incandela, M. Kilpatrick, J. Kim, B. Marsh, H. Mei, M. Oshiro, M. Quinnan, J. Richman, U. Sarica, F. Setti, J. Sheplock, P. Siddireddy, D. Stuart, S. Wang

California Institute of Technology, Pasadena, California, USA
A. Bornheim, O. Cerri, I. Dutta, J.M. Lawhorn, N. Lu, J. Mao, H.B. Newman, T.Q. Nguyen, M. Spiropulu, J.R. Vlimant, C. Wang, S. Xie, Z. Zhang, R.Y. Zhu

Carnegie Mellon University, Pittsburgh, Pennsylvania, USA
J. Alison, S. An, M.B. Andrews, P. Bryant, T. Ferguson, A. Harilal, C. Liu, T. Mudholkar, M. Paulini, A. Sanchez, W. Terrill

University of Colorado Boulder, Boulder, Colorado, USA
J.P. Cumalat, W.T. Ford, A. Hassani, G. Karathanasis, E. MacDonald, R. Patel, A. Perloff, C. Savard, N. Schonbeck, K. Stenson, K.A. Ulmer, S.R. Wagner, N. Zipper

Cornell University, Ithaca, New York, USA
J. Alexander, S. Bright-Thonney, X. Chen, Y. Cheng, D.J. Cranshaw, X. Fan, S. Hogan, J. Monroy, J.R. Patterson, D. Quach, J. Reichert, M. Reid, A. Ryd, W. Sun, J. Thom, P. Wittich, R. Zou

Fermi National Accelerator Laboratory, Batavia, Illinois, USA
M. Albrow, M. Alyari, G. Apollinari, A. Apresyan, A. Apyan, L.A.T. Bauerdick, D. Berry, J. Berryhill, P.C. Bhat, K. Burkett, J.N. Butler, A. Canepa, G.B. Cerati, H.W.K. Cheung, F. Chlebana, K.F. Di Petrillo, J. Dickinson, V.D. Elvira, Y. Feng, J. Freeman, A. Gandrakota, Z. Gecse, L. Gray, D. Green, S. Grünendahl, O. Gutsche, R.M. Harris, R. Heller, T.C. Herwig, J. Hirschauer, B. Jayatilaka, S. Jindariani, M. Johnson, U. Joshi, T. Klijnsma, B. Klima, K.H.M. Kwok, S. Lammel, D. Lincoln, R. Lipton, T. Liu, C. Madrid, K. Maeshima, C. Mantilla, D. Mason, P. McBride, P. Merkel, S. Mrenna, S. Nahn, J. Ngadiuba, V. Papadimitriou, N. Pastika, K. Pedro, C. Pena[65], F. Ravera, A. Reinsvold Hall[97], L. Ristori, E. Sexton-Kennedy, N. Smith, A. Soha, L. Spiegel, S. Stoynev, J. Strait, L. Taylor, S. Tkaczyk, N.V. Tran, L. Uplegger, E.W. Vaandering, H.A. Weber

University of Florida, Gainesville, Florida, USA
P. Avery, D. Bourilkov, L. Cadamuro, V. Cherepanov, R.D. Field, D. Guerrero, M. Kim, E. Koenig, J. Konigsberg, A. Korytov, K.H. Lo, K. Matchev, N. Menendez, G. Mitselmakher, A. Muthirakalayil Madhu, N. Rawal, D. Rosenzweig, S. Rosenzweig, K. Shi, J. Wang, Z. Wu, E. Yigitbasi, X. Zuo

Florida State University, Tallahassee, Florida, USA
T. Adams, A. Askew, R. Habibullah, V. Hagopian, K.F. Johnson, R. Khurana, T. Kolberg, G. Martinez, H. Prosper, C. Schiber, O. Viazlo, R. Yohay, J. Zhang

Florida Institute of Technology, Melbourne, Florida, USA
M.M. Baarmand, S. Butalla, T. Elkafrawy[16], M. Hohlmann, R. Kumar Verma, D. Noonan, M. Rahmani, F. Yumiceva

University of Illinois at Chicago (UIC), Chicago, Illinois, USA
M.R. Adams, H. Becerril Gonzalez, R. Cavanaugh, S. Dittmer, O. Evdokimov, C.E. Gerber, D.J. Hofman, A.H. Merrit, C. Mills, G. Oh, T. Roy, S. Rudrabhatla, M.B. Tonjes, N. Varelas, J. Viinikainen, X. Wang, Z. Ye

The University of Iowa, Iowa City, Iowa, USA
M. Alhusseini, K. Dilsiz[98], L. Emediato, R.P. Gandrajula, O.K. Köseyan, J.-P. Merlo, A. Mestvirishvili[99], J. Nachtman, H. Ogul[100], Y. Onel, A. Penzo, C. Snyder, E. Tiras[101]

Johns Hopkins University, Baltimore, Maryland, USA
O. Amram, B. Blumenfeld, L. Corcodilos, J. Davis, A.V. Gritsan, S. Kyriacou, P. Maksimovic, J. Roskes, M. Swartz, T.Á. Vámi

The University of Kansas, Lawrence, Kansas, USA
A. Abreu, J. Anguiano, C. Baldenegro Barrera, P. Baringer, A. Bean, Z. Flowers, T. Isidori, S. Khalil, J. King, G. Krintiras, A. Kropivnitskaya, M. Lazarovits, C. Le Mahieu, C. Lindsey, J. Marquez, N. Minafra, M. Murray, M. Nickel, C. Rogan, C. Royon, R. Salvatico, S. Sanders, E. Schmitz, C. Smith, Q. Wang, Z. Warner, J. Williams, G. Wilson

Kansas State University, Manhattan, Kansas, USA
S. Duric, A. Ivanov, K. Kaadze, D. Kim, Y. Maravin, T. Mitchell, A. Modak, K. Nam

Lawrence Livermore National Laboratory, Livermore, California, USA
F. Rebassoo, D. Wright

University of Maryland, College Park, Maryland, USA
E. Adams, A. Baden, O. Baron, A. Belloni, S.C. Eno, N.J. Hadley, S. Jabeen, R.G. Kellogg, T. Koeth, Y. Lai, S. Lascio, A.C. Mignerey, S. Nabili, C. Palmer, M. Seidel, A. Skuja, L. Wang, K. Wong

Massachusetts Institute of Technology, Cambridge, Massachusetts, USA
D. Abercrombie, G. Andreassi, R. Bi, W. Busza, I.A. Cali, Y. Chen, M. D'Alfonso, J. Eysermans, C. Freer, G. Gomez Ceballos, M. Goncharov, P. Harris, M. Hu, M. Klute, D. Kovalskyi, J. Krupa, Y.-J. Lee, K. Long, C. Mironov, C. Paus, D. Rankin, C. Roland, G. Roland, Z. Shi, G.S.F. Stephans, J. Wang, Z. Wang, B. Wyslouch

University of Minnesota, Minneapolis, Minnesota, USA
R.M. Chatterjee, A. Evans, J. Hiltbrand, Sh. Jain, B.M. Joshi, M. Krohn, Y. Kubota, J. Mans, M. Revering, R. Rusack, R. Saradhy, N. Schroeder, N. Strobbe, M.A. Wadud

University of Nebraska-Lincoln, Lincoln, Nebraska, USA
K. Bloom, M. Bryson, S. Chauhan, D.R. Claes, C. Fangmeier, L. Finco, F. Golf, C. Joo, I. Kravchenko, I. Reed, J.E. Siado, G.R. Snow†, W. Tabb, A. Wightman, F. Yan, A.G. Zecchinelli

State University of New York at Buffalo, Buffalo, New York, USA
G. Agarwal, H. Bandyopadhyay, L. Hay, I. Iashvili, A. Kharchilava, C. McLean, D. Nguyen, J. Pekkanen, S. Rappoccio, A. Williams

Northeastern University, Boston, Massachusetts, USA
G. Alverson, E. Barberis, Y. Haddad, Y. Han, A. Hortiangtham, A. Krishna, J. Li, J. Lidrych, G. Madigan, B. Marzocchi, D.M. Morse, V. Nguyen, T. Orimoto, A. Parker, L. Skinnari, A. Tishelman-Charny, T. Wamorkar, B. Wang, A. Wisecarver, D. Wood

Northwestern University, Evanston, Illinois, USA
S. Bhattacharya, J. Bueghly, Z. Chen, A. Gilbert, T. Gunter, K.A. Hahn, Y. Liu, N. Odell, M.H. Schmitt, M. Velasco

University of Notre Dame, Notre Dame, Indiana, USA
R. Band, R. Bucci, M. Cremonesi, A. Das, N. Dev, R. Goldouzian, M. Hildreth, K. Hurtado Anampa, C. Jessop, K. Lannon, J. Lawrence, N. Loukas, D. Lutton, J. Mariano, N. Marinelli, I. Mcalister, T. McCauley, C. Mcgrady, K. Mohrman, C. Moore, Y. Musienko[58], R. Ruchti, A. Townsend, M. Wayne, M. Zarucki, L. Zygala

The Ohio State University, Columbus, Ohio, USA
B. Bylsma, L.S. Durkin, B. Francis, C. Hill, M. Nunez Ornelas, K. Wei, B.L. Winer, B.R. Yates

Princeton University, Princeton, New Jersey, USA
F.M. Addesa, B. Bonham, P. Das, G. Dezoort, P. Elmer, A. Frankenthal, B. Greenberg, N. Haubrich, S. Higginbotham, A. Kalogeropoulos, G. Kopp, S. Kwan, D. Lange, D. Marlow, K. Mei, I. Ojalvo, J. Olsen, D. Stickland, C. Tully

University of Puerto Rico, Mayaguez, Puerto Rico, USA
S. Malik, S. Norberg

Purdue University, West Lafayette, Indiana, USA
A.S. Bakshi, V.E. Barnes, R. Chawla, S. Das, L. Gutay, M. Jones, A.W. Jung, D. Kondratyev, A.M. Koshy, M. Liu, G. Negro, N. Neumeister, G. Paspalaki, S. Piperov, A. Purohit, J.F. Schulte, M. Stojanovic[17], J. Thieman, F. Wang, R. Xiao, W. Xie

Purdue University Northwest, Hammond, Indiana, USA
J. Dolen, N. Parashar

Rice University, Houston, Texas, USA
D. Acosta, A. Baty, T. Carnahan, M. Decaro, S. Dildick, K.M. Ecklund, S. Freed, P. Gardner, F.J.M. Geurts, A. Kumar, W. Li, B.P. Padley, R. Redjimi, J. Rotter, W. Shi, A.G. Stahl Leiton, S. Yang, L. Zhang[102], Y. Zhang

University of Rochester, Rochester, New York, USA
A. Bodek, P. de Barbaro, R. Demina, J.L. Dulemba, C. Fallon, T. Ferbel, M. Galanti, A. Garcia-Bellido, O. Hindrichs, A. Khukhunaishvili, E. Ranken, R. Taus, G.P. Van Onsem

The Rockefeller University, New York, New York, USA
K. Goulianos

Rutgers, The State University of New Jersey, Piscataway, New Jersey, USA
B. Chiarito, J.P. Chou, Y. Gershtein, E. Halkiadakis, A. Hart, M. Heindl, O. Karacheban[25], I. Laflotte, A. Lath, R. Montalvo, K. Nash, M. Osherson, S. Salur, S. Schnetzer, S. Somalwar, R. Stone, S.A. Thayil, S. Thomas, H. Wang

University of Tennessee, Knoxville, Tennessee, USA
H. Acharya, A.G. Delannoy, S. Fiorendi, T. Holmes, S. Spanier

Texas A&M University, College Station, Texas, USA
O. Bouhali[103], M. Dalchenko, A. Delgado, R. Eusebi, J. Gilmore, T. Huang, T. Kamon[104], H. Kim, S. Luo, S. Malhotra, R. Mueller, D. Overton, D. Rathjens, A. Safonov

Texas Tech University, Lubbock, Texas, USA
N. Akchurin, J. Damgov, V. Hegde, K. Lamichhane, S.W. Lee, T. Mengke, S. Muthumuni, T. Peltola, I. Volobouev, Z. Wang, A. Whitbeck

Vanderbilt University, Nashville, Tennessee, USA
E. Appelt, S. Greene, A. Gurrola, W. Johns, A. Melo, K. Padeken, F. Romeo, P. Sheldon, S. Tuo, J. Velkovska

University of Virginia, Charlottesville, Virginia, USA
M.W. Arenton, B. Cardwell, B. Cox, G. Cummings, J. Hakala, R. Hirosky, M. Joyce, A. Ledovskoy, A. Li, C. Neu, C.E. Perez Lara, B. Tannenwald, S. White

Wayne State University, Detroit, Michigan, USA
N. Poudyal

University of Wisconsin - Madison, Madison, WI, Wisconsin, USA
S. Banerjee, K. Black, T. Bose, S. Dasu, I. De Bruyn, P. Everaerts, C. Galloni, H. He, M. Herndon, A. Herve, U. Hussain, A. Lanaro, A. Loeliger, R. Loveless, J. Madhusudanan Sreekala, A. Mallampalli, A. Mohammadi, D. Pinna, A. Savin, V. Shang, V. Sharma, W.H. Smith, D. Teague, S. Trembath-Reichert, W. Vetens

†: Deceased
1: Also at TU Wien, Wien, Austria
2: Also at Institute of Basic and Applied Sciences, Faculty of Engineering, Arab Academy for Science, Technology and Maritime Transport, Alexandria, Egypt
3: Also at Université Libre de Bruxelles, Bruxelles, Belgium
4: Also at Universidade Estadual de Campinas, Campinas, Brazil
5: Also at Federal University of Rio Grande do Sul, Porto Alegre, Brazil
6: Also at The University of the State of Amazonas, Manaus, Brazil
7: Also at University of Chinese Academy of Sciences, Beijing, China
8: Also at Department of Physics, Tsinghua University, Beijing, China
9: Also at UFMS, Nova Andradina, Brazil
10: Also at Nanjing Normal University Department of Physics, Nanjing, China
11: Now at The University of Iowa, Iowa City, Iowa, USA
12: Also at National Research Center 'Kurchatov Institute', Moscow, Russia
13: Also at Joint Institute for Nuclear Research, Dubna, Russia
14: Also at Cairo University, Cairo, Egypt
15: Also at British University in Egypt, Cairo, Egypt
16: Now at Ain Shams University, Cairo, Egypt
17: Also at Purdue University, West Lafayette, Indiana, USA
18: Also at Université de Haute Alsace, Mulhouse, France

19: Also at Tbilisi State University, Tbilisi, Georgia
20: Also at Erzincan Binali Yildirim University, Erzincan, Turkey
21: Also at CERN, European Organization for Nuclear Research, Geneva, Switzerland
22: Also at University of Hamburg, Hamburg, Germany
23: Also at RWTH Aachen University, III. Physikalisches Institut A, Aachen, Germany
24: Also at Isfahan University of Technology, Isfahan, Iran
25: Also at Brandenburg University of Technology, Cottbus, Germany
26: Also at Forschungszentrum Jülich, Juelich, Germany
27: Also at Physics Department, Faculty of Science, Assiut University, Assiut, Egypt
28: Also at Karoly Robert Campus, MATE Institute of Technology, Gyongyos, Hungary
29: Also at Institute of Physics, University of Debrecen, Debrecen, Hungary
30: Also at Institute of Nuclear Research ATOMKI, Debrecen, Hungary
31: Now at Universitatea Babes-Bolyai - Facultatea de Fizica, Cluj-Napoca, Romania
32: Also at MTA-ELTE Lendület CMS Particle and Nuclear Physics Group, Eötvös Loránd University, Budapest, Hungary
33: Also at Faculty of Informatics, University of Debrecen, Debrecen, Hungary
34: Also at Wigner Research Centre for Physics, Budapest, Hungary
35: Also at IIT Bhubaneswar, Bhubaneswar, India
36: Also at Institute of Physics, Bhubaneswar, India
37: Also at Punjab Agricultural University, Ludhiana, India
38: Also at UPES - University of Petroleum and Energy Studies, Dehradun, India
39: Also at Shoolini University, Solan, India
40: Also at University of Hyderabad, Hyderabad, India
41: Also at University of Visva-Bharati, Santiniketan, India
42: Also at Indian Institute of Science (IISc), Bangalore, India
43: Also at Indian Institute of Technology (IIT), Mumbai, India
44: Also at Deutsches Elektronen-Synchrotron, Hamburg, Germany
45: Now at Department of Physics, Isfahan University of Technology, Isfahan, Iran
46: Also at Sharif University of Technology, Tehran, Iran
47: Also at Department of Physics, University of Science and Technology of Mazandaran, Behshahr, Iran
48: Now at INFN Sezione di Bari, Università di Bari, Politecnico di Bari, Bari, Italy
49: Also at Italian National Agency for New Technologies, Energy and Sustainable Economic Development, Bologna, Italy
50: Also at Centro Siciliano di Fisica Nucleare e di Struttura Della Materia, Catania, Italy
51: Also at Scuola Superiore Meridionale, Università di Napoli Federico II, Napoli, Italy
52: Also at Università di Napoli 'Federico II', Napoli, Italy
53: Also at Consiglio Nazionale delle Ricerche - Istituto Officina dei Materiali, Perugia, Italy
54: Also at Riga Technical University, Riga, Latvia
55: Also at Department of Applied Physics, Faculty of Science and Technology, Universiti Kebangsaan Malaysia, Bangi, Malaysia
56: Also at Consejo Nacional de Ciencia y Tecnología, Mexico City, Mexico
57: Also at IRFU, CEA, Université Paris-Saclay, Gif-sur-Yvette, France
58: Also at Institute for Nuclear Research, Moscow, Russia
59: Now at National Research Nuclear University 'Moscow Engineering Physics Institute' (MEPhI), Moscow, Russia
60: Also at Institute of Nuclear Physics of the Uzbekistan Academy of Sciences, Tashkent, Uzbekistan
61: Also at St. Petersburg Polytechnic University, St. Petersburg, Russia

62: Also at University of Florida, Gainesville, Florida, USA
63: Also at Imperial College, London, United Kingdom
64: Also at P.N. Lebedev Physical Institute, Moscow, Russia
65: Also at California Institute of Technology, Pasadena, California, USA
66: Also at Budker Institute of Nuclear Physics, Novosibirsk, Russia
67: Also at Faculty of Physics, University of Belgrade, Belgrade, Serbia
68: Also at Trincomalee Campus, Eastern University, Sri Lanka, Nilaveli, Sri Lanka
69: Also at INFN Sezione di Pavia, Università di Pavia, Pavia, Italy
70: Also at National and Kapodistrian University of Athens, Athens, Greece
71: Also at Ecole Polytechnique Fédérale Lausanne, Lausanne, Switzerland
72: Also at Universität Zürich, Zurich, Switzerland
73: Also at Stefan Meyer Institute for Subatomic Physics, Vienna, Austria
74: Also at Laboratoire d'Annecy-le-Vieux de Physique des Particules, IN2P3-CNRS, Annecy-le-Vieux, France
75: Also at Şırnak University, Sirnak, Turkey
76: Also at Near East University, Research Center of Experimental Health Science, Nicosia, Turkey
77: Also at Konya Technical University, Konya, Turkey
78: Also at Piri Reis University, Istanbul, Turkey
79: Also at Adiyaman University, Adiyaman, Turkey
80: Also at Necmettin Erbakan University, Konya, Turkey
81: Also at Bozok Universitetesi Rektörlügü, Yozgat, Turkey
82: Also at Marmara University, Istanbul, Turkey
83: Also at Milli Savunma University, Istanbul, Turkey
84: Also at Kafkas University, Kars, Turkey
85: Also at Istanbul Bilgi University, Istanbul, Turkey
86: Also at Hacettepe University, Ankara, Turkey
87: Also at Istanbul University - Cerrahpasa, Faculty of Engineering, Istanbul, Turkey
88: Also at Ozyegin University, Istanbul, Turkey
89: Also at Vrije Universiteit Brussel, Brussel, Belgium
90: Also at School of Physics and Astronomy, University of Southampton, Southampton, United Kingdom
91: Also at Rutherford Appleton Laboratory, Didcot, United Kingdom
92: Also at IPPP Durham University, Durham, United Kingdom
93: Also at Monash University, Faculty of Science, Clayton, Australia
94: Also at Università di Torino, Torino, Italy
95: Also at Bethel University, St. Paul, Minneapolis, USA
96: Also at Karamanoğlu Mehmetbey University, Karaman, Turkey
97: Also at United States Naval Academy, Annapolis, N/A, USA
98: Also at Bingol University, Bingol, Turkey
99: Also at Georgian Technical University, Tbilisi, Georgia
100: Also at Sinop University, Sinop, Turkey
101: Also at Erciyes University, Kayseri, Turkey
102: Also at Institute of Modern Physics and Key Laboratory of Nuclear Physics and Ion-beam Application (MOE) - Fudan University, Shanghai, China
103: Also at Texas A&M University at Qatar, Doha, Qatar
104: Also at Kyungpook National University, Daegu, Korea